
The feasibility of a solid state type of refrigeration, which utilizes the electrocaloric effect in certain dielectric materials, has been investigated. The study was limited to the temperature range where the refrigerator would absorb heat from a load at about 4 K and reject heat to a reservoir at about 15 K. Heat switches would be required for such a refrigerator and two types were studied. One type was a multiple-leaf contact switch, the other a magnetothermal switch of single crystal beryllium. Many electrocaloric materials were studied but none was found with a sufficiently large reversible electrocaloric effect for a practical refrigerator. The largest effects were seen in a SrTiO₃ ceramic, followed by a KTaO₃ single crystal. Temperature reductions of about 0.3 K at 10 K were observed during depolarization from fields of 20 kV cm⁻¹. A theoretical model, based on the electret behaviour of impurity-vacancy dipoles is postulated to interpret the anomalous dielectric behaviour of the materials investigated. Another theoretical model, based on the lattice dynamics of displacive dielectrics, is postulated to explain the observed temperature changes seen in such materials. The model points out that at 4 K the entropies of displacive type materials are probably too low for practical refrigeration. An investigation of certain order-disorder dielectrics is suggested.

Key words: Beryllium; ceramics; cryogenics; dielectric-constant; electrets; electrocaloric effect; entropy; ferroelectrics; glass-ceramics; heat switches; magnetothermal conductivity; polarization; potassium tantalate; refrigeration; specific heat; strontium titanate.

Feasibility of electrocaloric refrigeration for the 4-15 K temperature range

R. Radebaugh, W.N. Lawless, J.D. Siegwarth and A.J. Morrow

Introduction

Purpose of work

The largest application of cryogenics in the region of 4 K is in the area of superconductivity. This application ranges from the low-power level devices employing the Josephson effect up to the large scale superconducting magnets and rotating machinery. These superconducting devices require temperatures below 15 K, and in most cases temperatures of about 4 K. In certain cases, infrared detection also requires 4 K temperatures or lower to improve sensitivity.

The unreliability of 4 K refrigerators has slowed the growth of applied superconductivity in commercial markets. A mean-time-between-failure (MTBF) of about 3000 h is a typical figure for such machines. Specialized mechanics are required to work on the refrigerators and their presence every few thousand hours serves as a reminder that 4 K is not easily achieved. Rotating compressors and expanders now offer some hope for a MTBF of about 10 000 h for large 4 K refrigerators. The Stirling cycle and Gifford-McMahon cycle refrigerators can also achieve a MTBF of 10 000 h even on a small size machine of about 1 W. Unfortunately, the regenerative heat exchangers used on such machines

become ineffective below about 10 K and in order to reach 4 K, a very reliable last stage is needed to span the gap between about 15 K and 4 K. In addition, this last stage should operate close to Carnot efficiency to maintain a good overall efficiency. A survey of cryogenic refrigerators¹ shows that 4 K refrigerators operate at the same fraction of Carnot efficiency as do 10-30 K refrigerators of the same power rating.

Preliminary studies² showed that a refrigerator utilizing the electrocaloric effect in certain glass-ceramic materials could make a promising last stage to span the gap between 15 K and 4 K. Since it is potentially a solid state type of device with no moving parts, the reliability of the electrocaloric refrigerator should far exceed that of the 15 K upper stage. Thus 4 K could be reached with the reliability of a 15 K regenerative type refrigerator.

The purpose of this project was to study the feasibility of an electrocaloric refrigerator which would absorb roughly 1 W at 4 K and reject the heat to a reservoir at about 15 K. Originally the refrigeration material was to have been a glass-ceramic of SrTiO₃. That choice was based on preliminary measurements and calculations² of the thermodynamic properties of research samples of SrTiO₃ glass-ceramics. These materials, developed by Lawless,³ show large changes in the ac dielectric constant with respect to temperature. Because of this behaviour, such a material has been used for low temperature capacitance thermometers³⁻⁵ and suggested for use as a low temperature bolometer.⁶ The same dielectric behaviour was the basis of a proposal^{2, 7} to use these SrTiO₃ glass-ceramics for an electrocaloric refrigerator.

R. Radebaugh and J.D. Siegwarth are with the Thermophysical Properties Division, National Bureau of Standards, Boulder, Colorado 80303, USA. W.N. Lawless was a guest worker at the Thermophysical Properties Division at the time this work was done. Both he and A.J. Morrow are presently with the Research and Development Laboratories, Corning Glass Works, Corning, New York 14830, USA. This research was supported by the Advanced Research Projects Agency of the Department of Defence and was monitored by ONR under Government Order Number NAonr-1-75. Received 1 December 1978.

This paper reviews and discusses measurements made to understand the dielectric and thermal behaviour exhibited by these materials. In addition, many other materials were investigated in order to evaluate the technical feasibility of electrocaloric refrigeration for the 4–15 K range.

Description of an electrocaloric refrigerator

Electrocaloric refrigeration is analogous to magnetic refrigeration, which is often referred to as adiabatic demagnetization.⁸ The difference is that in electrocaloric refrigeration the entropy of the working material is changed by an electric field rather than a magnetic field. The first experiments with the electrocaloric effect were on Rochelle salt by Kobeko and Kurtschatov⁹ in 1930. Since then electrocaloric effects in various materials have been studied, but not with the intent of using the electrocaloric effect for a refrigerator.

Quasicontinuous refrigeration is achieved by taking the refrigerating material through a closed loop on an entropy versus temperature diagram. Such a path is shown in Fig. 1. The entropy of the material is shown for four different values of electric field. If the material is at temperature T_2 in a field E_4 and the field is changed to E_2 , the material then cools adiabatically to the temperature T_1 . When going from the field E_2 to E_1 in an isothermal process, heat in the amount $Q_1 = T_1 \Delta S$ is absorbed. The change in field from E_1 to E_3 causes the sample to heat adiabatically to T_2 . An amount of heat $Q_2 = T_2 \Delta S$ is then rejected to a thermal reservoir at T_2 during the field change from E_3 to E_4 . The ratio of heat rejected at T_2 to the heat absorbed at T_1 is then simply the Carnot result $Q_2/Q_1 = T_2/T_1$ for the ideal cycle discussed here. If now two refrigerating elements are operated simultaneously such that at any time one or the other is in that part of the cycle where $T = T_1$, then

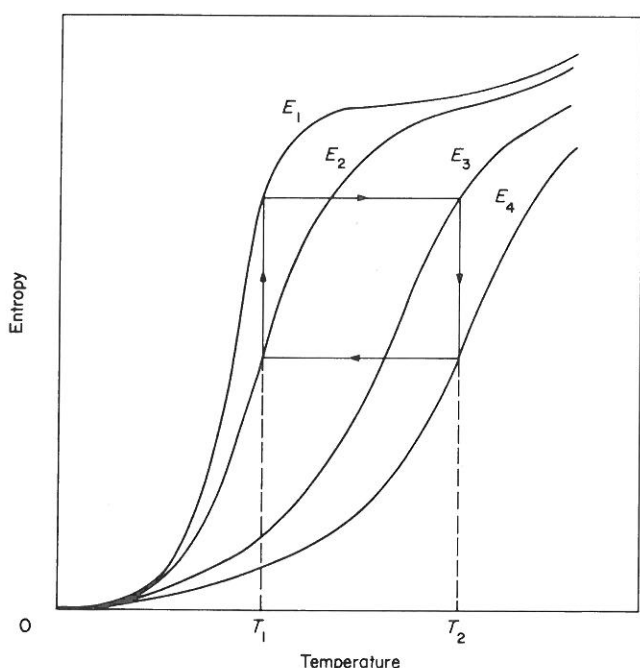


Fig. 1 Entropy vs temperature for different electric fields in a material useful for electrocaloric refrigeration. The ideal Carnot cycle, shown by the arrows, is traced out by changing the electric field from E_1 to E_3 to E_4 to E_2 and back to E_1

continuous refrigeration at T_1 is achieved.² Preliminary studies² indicated that cycle times of the order of 1 second should be optimum for a refrigerator of SrTiO₃ glass-ceramic operating between 4 and 15 K.

One conception of an electrocaloric refrigerator² capable of continuous refrigeration consisted of two half-cylinders of refrigeration materials. The two segments would operate 180° out of phase so that at any given time one segment is providing refrigeration at a temperature T_1 . Each half cylinder consisted of thin layers of the refrigeration material between an array of fins, which serve as electrodes and as a heat transfer device. The fins were connected to a copper post in the centre of each half-cylinder. These two copper posts could make thermal contact to the upper reservoir and the heat load by heat switches.

A rather unique magnetic refrigeration cycle was proposed by van Geuns¹⁰ which might be applied to the electrocaloric refrigerator. He suggested using high pressure helium gas as a regenerative material to help change the temperature of a paramagnetic (or paraelectric) material between 15 and 4 K. In that case the adiabatic lines in Fig. 1 are replaced by constant field lines. In the real cycle, however, there must be a small adiabatic segment at the end of the cooling or heating step to account for the finite ΔT required between the helium gas and the refrigeration material. With this regenerative cycle the heat load due to the lattice heat capacity is nearly eliminated from each cycle, but the initial cool down from 15 K is then done in very small steps until equilibrium is established in the helium gas. The helium gas must be at a high pressure (above the critical pressure) to provide a high heat capacity over a wide temperature range. The high pressure can pose certain mechanical problems in displacing the gas with respect to the refrigeration material. Whether this type of mechanical device would be any more reliable than a mechanical 4 K refrigerator can only be determined by experiment. We did not study this cycle in this project, instead, the heat switch approach has been studied here since it can be made with no moving parts.

Heat switches

Types of heat switches and minimum requirements

Two heat switches are required for the electrocaloric refrigerator, one to connect the cooling element with the 15 K reservoir, and the other to connect the cooling element with the 4 K load. The ratio of heat conducted in the 'on' state of the switch to that conducted in the 'off' case will be called the switch ratio and should be as high as possible. The switch ratio should probably be at least 30 to maintain a high refrigerator efficiency. In the 'off' condition, the switch must span the temperature difference between about 15 K and 4 K. In the 'on' case, the upper heat switch will be at about 15 K whereas the lower heat switch will be at 4 K. The temperature drop, ΔT across these switches in the 'on' case should be as small as possible. As a first approximation we take ΔT to be 1 K for both switches. For the refrigerator size considered in this project, the lower switch must then have an 'on' conductance of about 1 W K⁻¹ and the upper switch about 5 W K⁻¹. To achieve a switch ratio of 30 means

that the conductance ratio must be about $11 \times 30 = 330$ because the ΔT in the 'off' case is 11 times that of the 'on' case. These switches must be able to operate at roughly one cycle per second.

There are several ways in which the switch conductance can be varied with some external parameter. These parameters could be such things as force, gas pressure, magnetic field, or electric field. We know of no other parameters which could reversibly change the conductance of a heat switch. An electric-field controlled heat switch is especially attractive since electric fields are easy to establish and are already being used for the cooling element. Though the thermal conductivity of a material like SrTiO_3 can be changed with an electric field,¹¹ the effect is too small to make a useful heat switch.

Superconducting heat switches are commonly used for adiabatic demagnetization, but their use is restricted to temperatures below about 1 K. A large difference in the normal state and superconducting state thermal conductivity occurs only for temperatures far below the transition temperature. The operation of the switch requires a magnetic field to drive the material into the normal state. The mechanical switches commonly used in calorimetry¹² will operate in the 4–15 K temperature range, but their conductances are usually of the order of only a few milliwatts per kelvin instead of watts per kelvin.

Previously developed heat switches have been designed for lower temperatures, lower power levels, or longer cycle times than that required for this electrocaloric refrigerator. Hence, the programme included developments of proper heat switches. Two types were investigated and compared.

Mechanical heat switches

When two metal surfaces are pressed together in a vacuum, the heat transfer rate between them is proportional to F^n , where F is the total force acting on the surfaces and n is a number of the order of 0.7. Berman and Mate^{13, 14} measured the conductance of solid gold contacts at 4 K, they were closed at room temperature and found a value of 0.2 W K^{-1} for a 421 N closing force. The conductance decreased by about a factor of two when the force was applied at low temperatures. They found the conductance to be generally independent of the macroscopic surface area of the contacts. Since the conductances needed for a 1 W refrigerator would necessitate unreasonably large forces on a single contact heat switch, a multiple contact heat switch was developed for such a refrigerator. In this switch several gold-plated copper leaves intermesh with another set of leaves. A force F applied to the leaves acts on all contacts. For m contacts, the heat transfer rate is m times that of one contact with the same force F .

Several of these multiple contact heat switches were studied and reported in detail elsewhere.¹⁵ The number of contacts in these switches ranged from 2 to 13. From these tests it was found that conductances over 1 W K^{-1} could be achieved at 15 K with 10 contacts using a 490 N closing force. Switch ratios of about 1000 were obtained, but the use of many more contacts than 10 would seriously degrade the

switch ratio because of the difficulty in separating so many leaves for the off position.

Magnetothermal heat switches

The thermal conductivity of a metal is composed of the lattice and the electronic terms, ie $k = k_l + k_e$. The electronic contribution can be reduced considerably in many metals of high purity by the application of a transverse magnetic field. High-purity samples are required because the switch ratio is proportional to the residual resistance ratio (rrr). The reduction of electronic conductivity is proportional to the electrical magnetoresistive effect. Gallium has been used previously¹⁶ as a heat switch for the 1–4 K temperature range and existing data^{17, 18} on the magnetothermal conductivity of tungsten indicate that it would make a comparable heat switch. Switch ratios of the order of 100 would be possible for the lower switch which operates between the electrocaloric material and the 4 K load. Gallium and tungsten would not be satisfactory for the upper switch because the switch ratios would be too low.

Measurements of the magnetothermal conductivity of high-purity, single-crystal beryllium were made and are reported in detail elsewhere.¹⁹ Fig. 2 shows how the thermal conductivity along the hexagonal c axis of single crystal beryllium depends on the temperature and magnetic field along the a axis. Early data of Gruneisen and Adenstedt²⁰ are shown in comparison. It is evident in Fig. 2 that large switch ratios are possible with beryllium for temperatures as high as 20–30 K using magnetic fields of 955 kA m^{-1} (12 KOe).

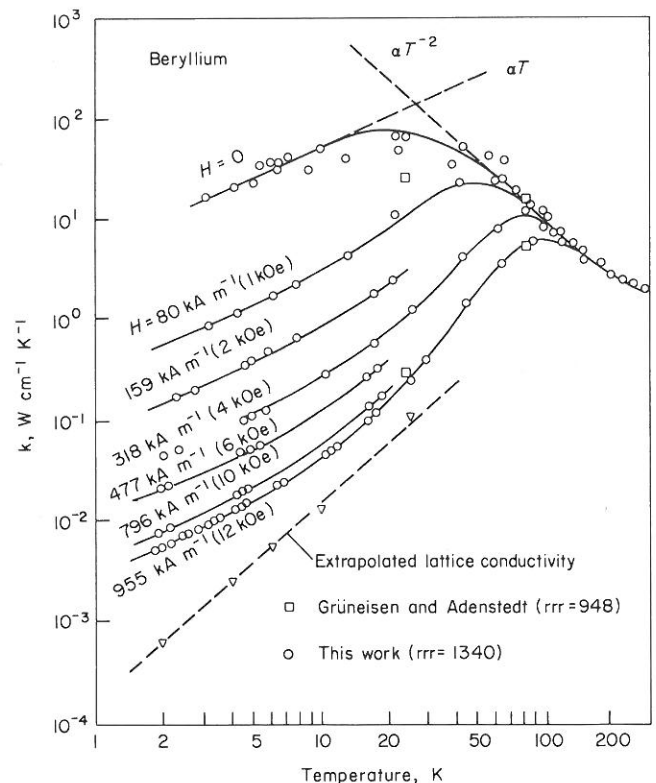


Fig. 2 The thermal conductivity of high purity single crystal beryllium as a function of temperature for various transverse magnetic fields

High purity copper or Nb₃Sn wire would be needed for the coil to establish the magnetic field at 15 K with little or no heat dissipation. A small iron yoke can be used to confine the transverse field to the region just around the beryllium sample. Further study is needed to determine how fast the field could be cycled.

Thermodynamics of electrocaloric refrigeration

The general TdS equation for a dielectric material is

$$TdS = C_E dT + T(\partial P/\partial T)_E dE, \quad (1)$$

where T is the temperature, S is the entropy per unit volume, C_E is the specific heat per unit volume in the electric field E , and P is the polarization of the sample. The refrigeration absorbed per unit volume during the isothermal step from E_2 to E_1 in Fig. 1 is given by

$$Q_L = T_1 \Delta S = T_1 \int_{E_2}^{E_1} (\partial P/\partial T)_E dE. \quad (2)$$

In the adiabatic process, temperature changes are given by

$$\frac{dT}{dE} = -\frac{T}{C_E} \left(\frac{\partial P}{\partial T} \right)_E \quad (3)$$

The temperature change during the adiabatic step from E_4 to E_2 is best determined by equating the entropy changes along a fictitious path from E_4 to E_2 at the temperature T_2 and then from T_2 to T_1 along the field line E_2 . These entropy changes are given by

$$\int_{T_1}^{T_2} \left(\frac{C_E}{T} \right)_{E_2} dT = \int_{E_4}^{E_2} (\partial P/\partial T)_{T_2} dE. \quad (4)$$

The specific heat in an electric field is given by²¹

$$C_E = C_0 + T \int_0^E \left(\frac{\partial^2 P}{\partial T^2} \right)_E dE, \quad (5)$$

where C_0 is the specific heat in zero field. Equations (2) to (5) point out the fact that the thermodynamic behaviour of a dielectric material can be determined entirely from $C_0(T)$ and $P(T, E)$. This fact can be visualized by considering the entropy in Fig. 1 as a surface in (T, E) space. The entropy at a point (T_1, E_1) is found by integrating (1) from $(0, 0)$ where $S = 0$. One may choose any integration path, but the path considered here follows the $E = 0$ plane from $T = 0$ to $T = T_1$ and then along the T_1 plane from $E = 0$ to $E = E_1$. Each of the two segments of the path use only one of the terms in (1) because first the field is held constant and then the temperature is held constant. The total entropy is then given as

$$S(T_1, E_1) = \int_0^{T_1} \frac{C_0}{T} dT + \int_0^{E_1} \left(\frac{\partial P}{\partial T} \right)_{T_1, E} dE \quad (6)$$

The permittivity ϵ of a dielectric is given as $\epsilon = \epsilon_0 + (\partial P/\partial E)_T$ so that the polarization can be derived from the relative dielectric constant by the expression

$$P(T, E) = \epsilon_0 \int_0^E [K'(T, E') - 1] dE' + P(T, 0), \quad (7)$$

where ϵ_0 is the permittivity of free space and K' the relative dielectric constant. The last term accounts for any remanent

polarization in the material. A material with any remanent polarization is normally referred to as pyroelectric. If the direction of polarization can be reversed, then it is called a ferroelectric. During the course of this programme another source of remanent polarization was discovered in almost all the materials studied. This is called the thermal electret effect, where a sample cooled down in an electric field will have a frozen in remanent polarization. The electret effect will be discussed in more detail later.

The temperature-entropy diagram of a dielectric material can also be determined entirely from specific heat measurements without recourse to polarization measurements. This can be done by choosing the integration path for (1) to be first along the $T = 0$ plane from $E = 0$ to $E = E_1$ and then along the E_1 plane from $T = 0$ to $T = T_1$. In that case, the total entropy is given as

$$S(T_1, E_1) = \int_0^{E_1} \left(\frac{\partial P}{\partial T} \right)_{T=0} dE + \int_0^{T_1} \frac{C_{E_1}}{T} dT, \quad (8)$$

which must be the same as that derived from any other path. The third law of thermodynamics requires $S = 0$ at $T = 0$, so that the first term for $S(T_1, E_1)$ must be zero, ie $(\partial P/\partial T)_{E=0} = 0$ at $T = 0$. The entropy in any electric field is then simply given as

$$S(T, E) = \int_0^T \frac{C_E}{T'} dT'. \quad (9)$$

To use this type of expression for the entropy requires measurements of the specific heat in electric fields down to temperatures much less than T_1 in Fig. 1. In that case, the uncertainty in the entropy due to the extrapolation of the specific heat down to 0 K is usually negligible. Equation (9) includes the lattice entropy, so that field-induced entropy changes which are small compared with the lattice entropy would be difficult to detect from (9). For that reason, and because specific heat measurements are time consuming, polarization measurements were used more often in this work to find ΔS upon a field change via (2). The uncertainty in ΔS determined from $\partial P/\partial T$ is unaffected by the size of the lattice entropy.

Large entropy changes upon a change in the field will occur at temperatures not too far removed from a transition. The entropy curves shown in Fig. 1 are indicative of a zero field transition near T_1 . Such a transition in a dielectric could be associated with a change from a ferroelectric or antiferroelectric state to the paraelectric state. The minimum entropy change required at T_1 can be roughly estimated. In going from T_2 to T_1 in Fig. 1, the dielectric material must be able to cool itself as well as metallic heat conductors and any inactive dielectric. If we assume that the metallic parts and the inactive dielectric occupy about 10% of the total volume of the refrigeration material, then the entropy change in the active dielectric would be on the order of $1 \text{ mJ K}^{-1} \text{ cm}^{-3}$ in cooling down the other materials from 15 K to 4 K. At 15 K, the lattice entropy of the active dielectric would also be about $1 \text{ mJ K}^{-1} \text{ cm}^{-3}$. Therefore, the entropy available at T_1 needs to be somewhat larger than $2 \text{ mJ K}^{-1} \text{ cm}^{-3}$ if any isothermal refrigeration is to be performed. In terms of the gas constant we require $S_4 \geq 10^{-2}R$. If the cool down from 15 K to 4 K

is to be done in a regenerative mode¹⁰ or in several stages instead of one, then the entropy of a material at 4 K can be smaller than $10^{-2}R$ and yet still be able to cool itself from 15 K to 4 K.

Refrigeration materials

Previous work

The first measurements⁹ of the electrocaloric effect were done in 1930, only four years after the first measurements²² of the magnetocaloric effect. The magnetocaloric effect was used for adiabatic demagnetization below 1 K within a few years after the first measurements. However, further work on the electrocaloric effect was not done until some twenty years later, probably because so little was known at that time of the dielectric behaviour of materials. After the ferroelectric state was better understood, several more measurements²³ of the electrocaloric effect were made on such materials, but always near room temperature. Granicher²⁴ first suggested the use of SrTiO₃ for electrocaloric cooling at low temperatures. His suggestion was based on his dielectric constant measurements of SrTiO₃. The dielectric constant of this material has a large negative temperature derivative around 20 K, even though it does not become ferroelectric. At 3 K and below²⁵ the dielectric constant of SrTiO₃ is independent of temperature. The behaviour is consistent with Barrett's theory²⁶ which means that no transition to the ferroelectric state occurs.

Hegenbarth²⁷ was the first to make electrocaloric effect measurements on SrTiO₃, which in that case were ceramic samples. With an electric field of 8 kV cm^{-1} , he saw adiabatic depolarization cooling of 6 mK at 78 K and 60 mK cooling at 17.5 K. Somewhat larger effects were seen in later measurements^{28, 29} on single crystal SrTiO₃, but these cooling effects disappeared below about 4–5 K. Cooling effects at higher electric fields could be significantly higher, but were not tried because of the problem of breakdown in the samples. The temperature changes observed in the single crystal SrTiO₃ were in reasonable agreement with values calculated from the specific heat and the observed dielectric constant versus temperature and electric field.^{28, 30} The uncertainty in the calculation was dominated by that of the specific heat, since no accurate specific heat data existed in the liquid helium temperature range.

Electrocaloric cooling at still lower temperatures was first demonstrated in OH doped KCl by three independent investigations.^{31–33} Cooling to 0.36 K from a starting temperature of 1.3 K was reported.³³ Various theoretical studies^{21, 34} and experimental investigations^{35, 36} on other doped halides followed shortly. Cooling to as low as 0.05 K was demonstrated in CN doped RbCl.³⁶ Electrocaloric refrigeration using KCl : OH has been used³⁷ for thermostating crystal below 1 K while they were radiated with short light pulses. Patents have been issued^{38, 39} for electrocaloric refrigeration with doped alkali halides as the refrigerant.

Lang⁴⁰ recently proposed the use of pyroelectric lithium sulphate monohydrate for refrigeration below about 2 K. His calculations are based on measurements⁴¹ above 4 K of the pyroelectric coefficient π ($\pi = \partial P_S / \partial T$, where P_S is the

spontaneous polarization) and on the assumption that π is linear in T . He predicts rather large cooling effects when a field of 100 kV cm^{-1} is applied. However, the third law of thermodynamics can be used to show⁴² that π must be proportional to at least T^3 whenever c_0 is proportional to T^3 rather than T as used by Lang.⁴⁰ When this fact is taken into account, the calculated temperature changes will be smaller.

Of all the materials studied previously, none showed large enough electrocaloric effects in the fields used to be useful as a refrigerator in the 4–15 K temperature range. The doped alkali halides appear to be quite powerful for temperatures below 1 K. However, because these materials usually contain only about 10^{18} – 10^{19} impurities per cm^3 , they do not have enough cooling power to cool the lattice significantly in the 4–15 K range. An increase in the impurity concentration would be most useful if it can be done without clustering. The existing studies on SrTiO₃ (single crystal and ceramic) indicated that this type of material was better suited at present for cooling at higher temperatures than the doped alkali halides. The large positive slopes seen in the dielectric constant versus temperature at 4 K for the SrTiO₃ glass-ceramics³ suggested that these materials would have larger cooling effects at 4 K than ceramic or single crystal SrTiO₃.

Criteria for materials selection

The thermodynamic groundwork previously developed was used to establish the criteria for selecting materials to try for electrocaloric cooling effects. Originally it was thought that the $P(T, 0)$ term in (7) would be zero or negligibly small for a paraelectric or antiferroelectric material. In that case the ac dielectric constant could be used to find $P(T, E)$ and the related thermodynamic properties. From (1) it is evident that large refrigeration effects require a large $\partial K' / \partial T$. The original set of criteria for material selection was the following: a large zero field $\partial K' / \partial T$ in the 4–15 K temperature range; the term $\partial K' / \partial T$ must remain sufficiently high up to the maximum field to be used; a high breakdown strength to provide wide limits of integration in (2); negligible hysteresis in $K'(T, E)$; and the phonon dipole relaxation time be much less than 1 s. Preliminary experimental results on research samples and on small plant manufactured samples of SrTiO₃ glass-ceramics indicated that all these conditions could be met.² However, only the plant manufactured multilayer samples could give the high breakdown strengths.

As will be discussed in more detail later, ac dielectric constant measurements were replaced with dc polarization measurements in most cases. In addition to searching for materials which would meet the criteria, various measurements were made on certain materials to understand the dielectric and thermal behaviour of dielectric materials. In general the materials studied had high dielectric constants which showed a temperature dependence near 4 K. Several of the materials chosen were reported in the literature to have a transition to either the ferroelectric or antiferroelectric state in the vicinity of 4–15 K. Various solid solutions in SrTiO₃ and KTaO₃ were tried in hopes that such solutions may lower the temperature at which the dc polarization still shows a temperature dependence.

Fabrication methods

SrTiO₃ glass ceramics. These glass ceramics are select compositions in the SrO-TiO₂-Nb₂O₅-Al₂O₃-SiO₂ system, where Al₂O₃-SiO₂ component is the glass phase. The SiO₂/Al₂O₃ ratio varies from approximately 3 to 4. The composition is heated to a range of 900–1300°C, which is called the ceram temperature. When held at this temperature for a period of time, SrTiO₃ crystals of about 5–10 μm size are formed in the glass solution. The SrTiO₃ component constitutes on the order of 50 volume % of the total solution. The solution is then cooled slowly to room temperature. The Nb₂O₅ component is usually added to the system to produce a SrNb₂O₆ doping of about 2 mol %. This doping increases the temperature derivative of the dielectric constant at 4 K. The reader is referred to the literature^{43, 44} for a more detailed account of the preparation of these materials. Preliminary work was done on bulk samples ground down into thin sheets with electrodes attached to each face.² The problem with such samples was that microcracks through the material resulted in a rather small dielectric breakdown strength.

To test the properties of these glass-ceramics at high field strengths required that multilayer samples be made according to a Corning Glass Works capacitor fabrication process. Essentially it consists of alternate layers of glass-ceramic (~ 0.03 mm thick) and precious metal electrodes sealed under heat and pressure to form a monolithic unit. The first step was to ball mill ribbons of uncrystallized glass in water to a size of 2.75 μm. The powder was dried and then mixed with an aqueous binder system. After some more ball milling and de-airing the slurry was cast into a thin film about 28 μm thick. In order to produce capacitors, a wet stacking method was used in which electrodes were silk-screened onto the dielectric film. The screen was shifted after each application to effectively produce several capacitors in parallel. The electrodes (3.8 μm thick) were usually made from a Pd-Pt-Au paste with 6 weight percent glass frit added. In later samples two or three layers of dielectric were placed on top of each other before depositing an electrode layer. This procedure made it highly unlikely that a pinhole in the dielectric could extend from one electrode to another, reducing the probability of shorts and increasing the resistance to breakdown under voltage. The stack was made about 0.84 mm thick.

The first step in the heating cycle was to burn out the organic binder at about 350°C for 20 hours. The temperature was slowly increased to about 915°C with a pressure of about 7 atmospheres applied to the sample. The stack was cooled slowly to room temperature and then cut into 25 samples of 1.9 cm x 1.9 cm. These samples were then heated to a ceram temperature in the range of 1000–1300°C with a 400 g weight on each sample to prevent curling. After firing, the ends of the samples were ground to insure good electrode exposure. A silver paste was applied to the electrode edges and fired at 620°C for 10 minutes. Many of the process variables, such as composition, ceram temperature, time at ceram temperature, etc, were varied to optimize the temperature derivative of the dielectric constant at 4 K and the breakdown strength.

Ceramics. After the irreversible heating effect was observed in glass-ceramic samples, it was decided to eliminate the glass matrix and make pure ceramic samples. At first, only the strontium titanate and potassium tantalate systems were attempted. Later, however, solid solutions of other oxides in the above systems and new compositions in the lead-pyroniobate family were made.

The following general procedure was used in the preparation of all ceramic compositions:

1. The composition was calculated in weight percent from the chemical formula;
2. Using a '00' size porcelain ball mill with porcelain media, the reagent grade powders were ground for 6 h at a speed of 73 rpm (loading was 350 g powder to 350 ml of liquid media either methanol, water or acetone).
3. The mixture was dried and ground with a mortar and pestle, then put into ZrO₂ saggars and calcined;
4. The calcined material was reground in the mortar and pestle.

At this stage two different procedures were followed in making the final samples, depending upon the chemical compatibility of the ceramic with the aqueous batch and the expected volatility of the ceramic during firing. One procedure was to make multilayer samples from films of the powder and an aqueous binder. These samples were made with laminates of 20 films, each 33 μm thick. After the samples were fired, electrodes were applied by firing a silver paste to both sides of the sample. The other procedure followed for some samples was to mix 5% by weight carbowax, dissolved in acetone, to the powder. Pellets, 9.5 mm diameter were then pressed from 3 g of the material. After firing, the pellets were sliced using a diamond saw. Silver electrodes were then applied to these samples. Further details regarding fabrication techniques are given elsewhere.^{44, 45}

Borrowed samples. Ceramic samples of the PbZr_xTi_{1-x}O₃ (PZT) system were obtained from G. Samara of Sandia Laboratories. Samples of 95/5 and 65/35 PZT were obtained for this programme. Likewise a high quality single crystal of KTaO₃ was kindly loaned to us by G. Samara. This sample was the same one measured by Samara and Morosin⁴⁶ and showed no strain birefringence at room temperature. The major faces of the crystal were [100] faces and were electroded with a small amount of silver paste.

Experimental methods

Dielectric properties

Dielectric constant and derivative. The quantity $(\partial K'/\partial T)_{E=0}$ was the main property of the multilayer samples to be tested. Such measurements had to be made on hundreds of these samples to test the effects of various manufacturing procedures. A cryostat insert was made whereby a fifteen sample teflon holder was mounted on the end of the stainless steel tube. The holder was immersed in a bath of liquid helium which could be pumped down to about 1.5 K.

A germanium thermometer was used to measure the temperature of the helium bath, which was controlled with a manostat. Each of the fifteen samples were connected in turn to a commercial capacitance bridge operating at 1 KHz. The capacitance of each sample was measured at 4.2 K and at a few lower temperatures. The data were computer analyzed to find K' and $\partial K'/\partial T$ for each sample.

For measurements of the dielectric constant at temperatures above 4 K, the specific heat apparatus was used. In that apparatus (described in the next section) only two samples could be run at the same time.

Breakdown strength at 4 K. The breakdown strengths of the glass ceramic capacitors were measured at 4 K in liquid helium. The dewars used were unsilvered so any external breakdown could be observed. A 1.5 M Ω current limiting resistor was placed in series with the capacitor. As the voltage on the sample was increased, the leakage current was monitored. Currents of about 1 μ A could be detected.

dc polarization. As shown earlier in the section on thermodynamics, the polarization $P(T, E)$ is used to determine the refrigeration power. When a remanent polarization is present, $P(T, E)$ can no longer be determined from the dielectric constant, but must be measured directly with a dc technique.

A circuit was made⁴⁷ to measure both $P(T)$ and $P(E)$ which was similar to that used by Gesi.⁴⁸ Basically a capacitance technique is used in which the dc voltage across a large known capacitance in series with the sample capacitance is measured after a voltage is applied. The precision of the measurement is about 0.01% for the larger capacitors measured. The total polarization P_t and the remanent polarization P_r could be measured with this circuit.

Thermodynamic properties

The various thermodynamic properties of interest are the field dependent specific heat $C_E(T)$, the electrocaloric coefficient, $\beta_E(T) = (\partial T/\partial E)_S$, and the state function $(\partial P/\partial T)_E$. All three of these quantities were measured simultaneously in the specific heat apparatus described in detail elsewhere.^{44, 49} The sample is connected by a weak thermal link (carbon resistor) to a reservoir. The specific heat of the sample is first measured in zero field. The conductance of the thermal link is then determined by observing the thermal time constant of the sample. Next, the field dependent properties are measured by applying a field change ΔE about E . The induced temperature change ΔT gives the electrocaloric coefficient, $\beta_E(T)$, and the thermal time constant gives the field dependent specific heat, $C_E(T)$. The state function is then given by

$$(\partial P/\partial T)_E = -C_E \beta_E / T. \quad (10)$$

Corrections for the addenda (including inactive dielectric) heat capacity are made, but these corrections cancel in the calculation of $(\partial P/\partial T)_E$ from (10). The addenda heat capacity amounted to about 4% of that of the sample above 10 K and about 20% at 2 K. The sample thermometers were 1/8 W, 220 Ω carbon thermometers calibrated against a germanium resistance thermometer mounted on the reservoir. The measurements of specific heat and electrocaloric coefficient are accurate to within about 5%.

Experimental results

SrTiO₃ glass-ceramics

The dielectric constant for a typical SrTiO₃ glass-ceramic as a function of temperature is shown in Fig. 3. The value of $\partial K'/\partial T$ at 4 K was as high as 25 K⁻¹ for some research samples. For the multilayer samples manufactured in the plant, the maximum $\partial K'/\partial T$ at 4 K was about 3.5 K⁻¹. Breakdown strengths of the multilayer samples were about 550 kV cm⁻¹. The specific heat of an unelectroded multilayer-sample is shown in Fig. 4. Unfortunately data could not be obtained at temperatures where there was a peak in the dielectric constant. If the peak was due to a transition, then the specific heat would also have shown anomalous behaviour around that temperature. Shown for comparison in Fig. 4 is the specific heat of single crystal SrTiO₃⁵⁰ and fused SiO₂. The SrTiO₃ glass-ceramic specific heat lies between the two, which would be expected for a mixture of SrTiO₃ and SiO₂. Measurements on electroded multilayer samples gave similar results. With an electric field of 220 kV cm⁻¹ the specific heat decreased less than about 5% compared with the zero field specific heat.

Measurements of the electrocaloric effect on two multilayer samples showed only heating effects for temperatures around 4 K. The heating occurred with both a field increase or a field decrease. The results of one such run are shown in Fig. 5. From this figure it can be seen that less heating occurs during a field decrease. This suggests that there may be a reversible electrocaloric effect which is dominated by

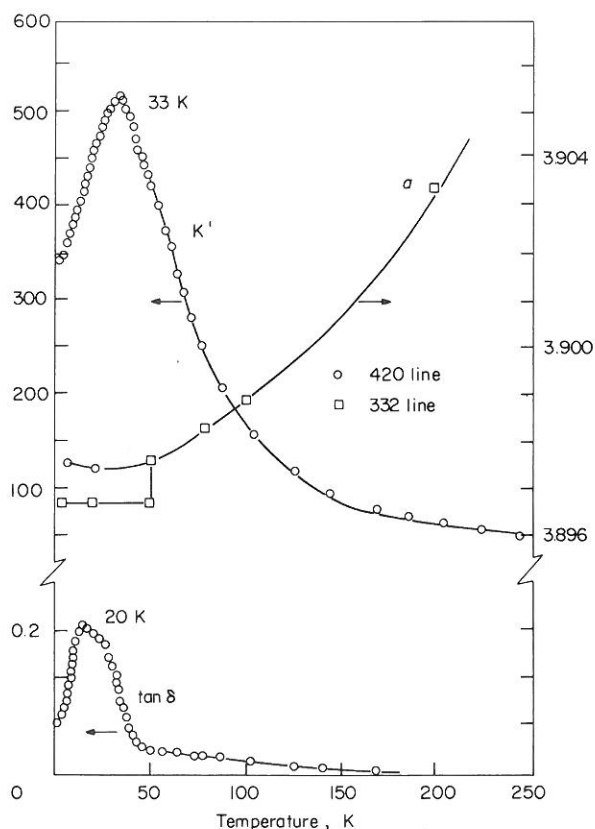


Fig. 3 Dielectric constant (K'), dielectric loss ($\tan \delta$) and lattice parameter data (a) measured on a SrTiO₃ glass ceramic from 2 to 250 K. The Curie-Weiss behaviour of K' extends to, and above, room temperature

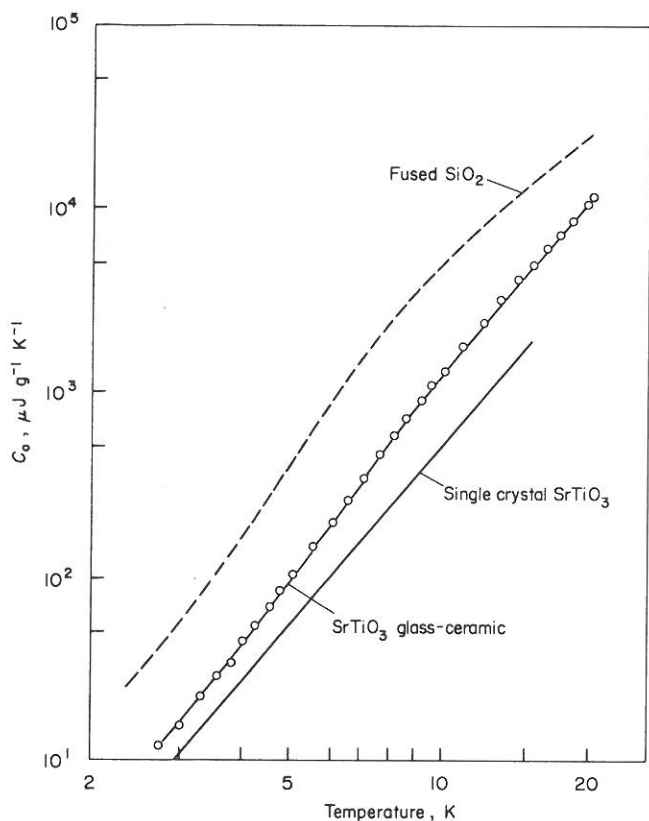


Fig. 4 Specific heat of an unelectroded SrTiO₃ glass-ceramic sample compared with fused SiO₂ and single crystal SrTiO₃.

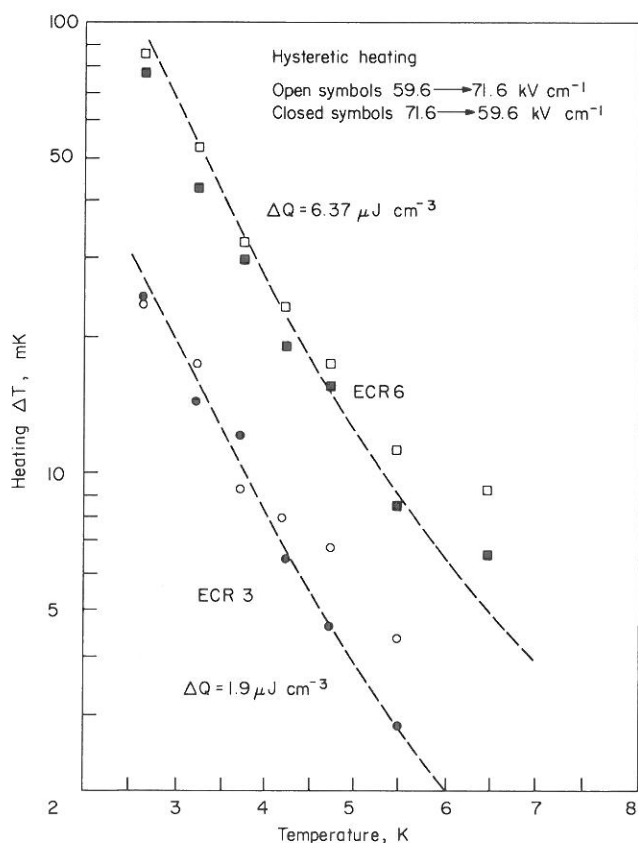


Fig. 5 The temperature rise in two previously polarized SrTiO₃ glass-ceramic samples during a change in the electric field. The open symbols are for an increase in field and the closed symbols are for a decrease in field

hysteretic heating. That particular electrocaloric effect, however, is extremely small and is of the opposite sign to that expected from the positive $\partial K'/\partial T$ at 4 K. Electrocaloric effects at temperatures between 20 and 40 K are shown in Fig. 6. Here the reversible electrocaloric effect dominates hysteretic heating. Unfortunately the cooling effect of 20 mK at 30 K for a field change from 120 kV cm⁻¹ to 0 is much too small to be of any practical use. These electrocaloric measurements would suggest a negative value of $\partial P/\partial T$ for all temperatures below 40 K. In contrast, the positive $\partial K'/\partial T$ suggested that $\partial P/\partial T$ would be positive.

Direct measurements of $P(T)$ were undertaken to resolve the conflicting behaviour of the dielectric constant and the electrocaloric effect. Fig. 7 and Table 1, shows the results of some of these measurements made on four SrTiO₃ glass-ceramic samples with varying composition. The samples used for the electrocaloric effect measurements were similar to that of sample 2 in Fig. 7. Detailed discussions of the polarization results are given elsewhere.⁵¹ The important points to note from these results are the fact that the total polarization P_t has a negative slope at all temperatures and the fact that there exists a remanent polarization, P_r .

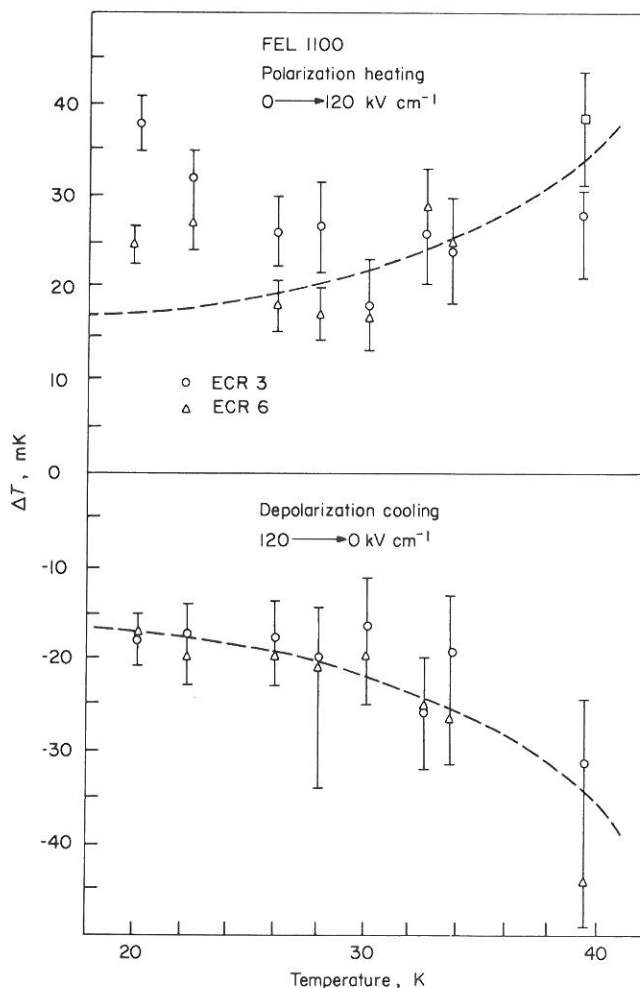


Fig. 6 The temperature change in two previously polarized SrTiO₃ glass-ceramic samples during a change in the electric field. These data are for the 20-40 K temperature range where cooling is seen for a decrease in field

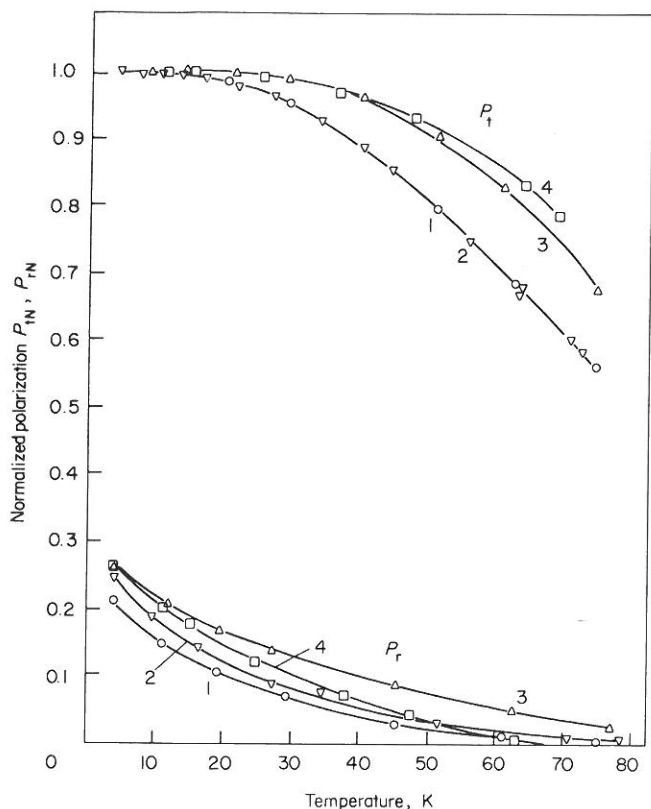


Fig. 7 Curves of normalized total polarization, P_t and remanent polarization, P_r as a function of temperature for four glass-ceramic samples of differing composition but with similar crystallization temperatures

Table 1. Direct measurements of $P(T)$ taken for four samples of SrTiO_3 glass ceramic samples

Sample No	E , kV cm^{-1}	$P_t(4\text{K})$, $\mu\text{C cm}^{-2}$
1	3.6	0.113
2	3.7	0.141
3	3.6	0.094
4	7.1	0.12

The remanent polarization occurs when the field is applied at a high temperature and removed at 4 K and then the sample is heated up to the measuring temperature. The total polarization was measured by applying the field at 77 K and then reducing the temperature. Fields of about 4 kV cm^{-1} were used for the measurements. The behaviour of P_t measured here was consistent with the electrocaloric measurements. There is negligible slope in the P_t curve at 4 K and so the expected electrocaloric effect at that temperature would be very small. Measurements of P_t were also made by applying the field at 4 K and then warming the sample. Those results showed a peak in P_t at temperatures of about 25 K. The explanation for such behaviour is given later on.

SrTiO_3 Ceramics

The dielectric constant of nominally pure SrTiO_3 ceramic was nearly independent of temperature below 6 K and had the value $K' = 6500$. This behaviour is in qualitative agreement with that of single crystal samples.⁵² However, when a small

amount (2–20%) of vanadium was added to these samples the dielectric constant showed peaks at temperatures of about 30–40 K, similar to that of the glass ceramics. Details of these measurements as well as polarization measurements are given elsewhere.^{44, 47} In essence, the polarization curves, shown in Fig. 8, are similar to those for the SrTiO_3 glass ceramics, except that the magnitudes of P_t and $\partial P_t / \partial T$ per unit field are larger for the ceramics.

Results of the specific heat and electrocaloric measurements on a high purity SrTiO_3 ceramic have been published by Lawless and Morrow.⁵³ Electrocaloric cooling effects in the pure SrTiO_3 ceramics were about an order of magnitude larger than those in the glass-ceramics. As shown in Fig. 9, cooling effects of about 0.3 K at 10 K occurred when the sample was depolarized from a field of 20 kV cm^{-1} . Unfortunately, higher fields caused sample breakdown. Cooling effects in the vanadium doped samples were less than those of the pure SrTiO_3 ceramics, in agreement with that expected from polarization measurements.^{44, 47} Of all the materials tested in this programme the largest cooling effects were seen in the pure SrTiO_3 ceramics.

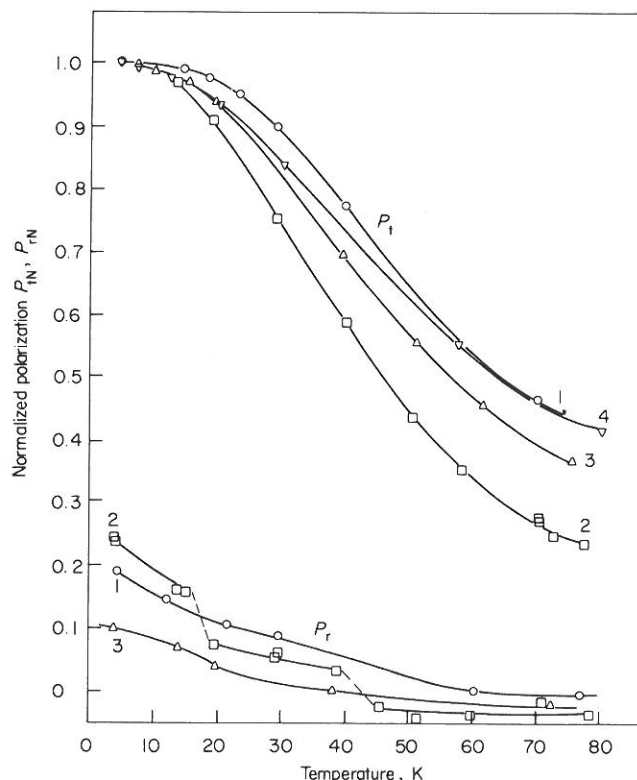


Fig. 8 Curves of normalized total polarization and remanent polarization as a function of temperature for various SrTiO_3 ceramic samples

Table 2. Direct measurements of $P(T)$ taken for four samples of SrTiO_3 ceramic

Sample No	E , kV cm^{-1}	$P_t(4\text{K})$, $\mu\text{C cm}^{-2}$
1 commercial grade	0.53	0.21
2 CP grade	0.46	0.33
3 CP grade	0.39	0.064
4 Nominally pure	0.34	0.068

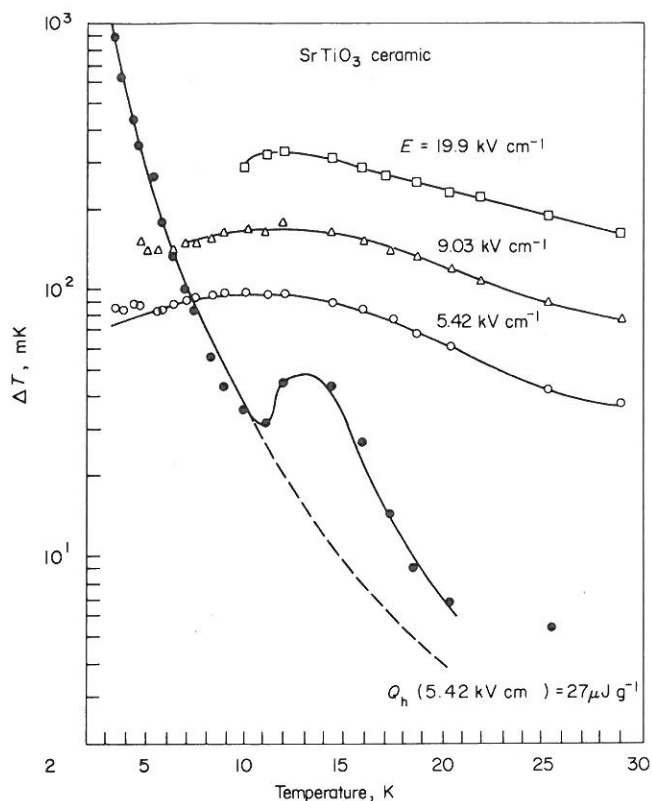


Fig. 9 Typical electrocaloric data measured on the SrTiO₃ ceramic sample No 2.⁵³ The open symbols represent the reversible component and the full symbols represent the irreversible component for 5.42 kV cm⁻¹. Note that at this field strength, no cooling effects are seen for $T \lesssim 7.4$ K

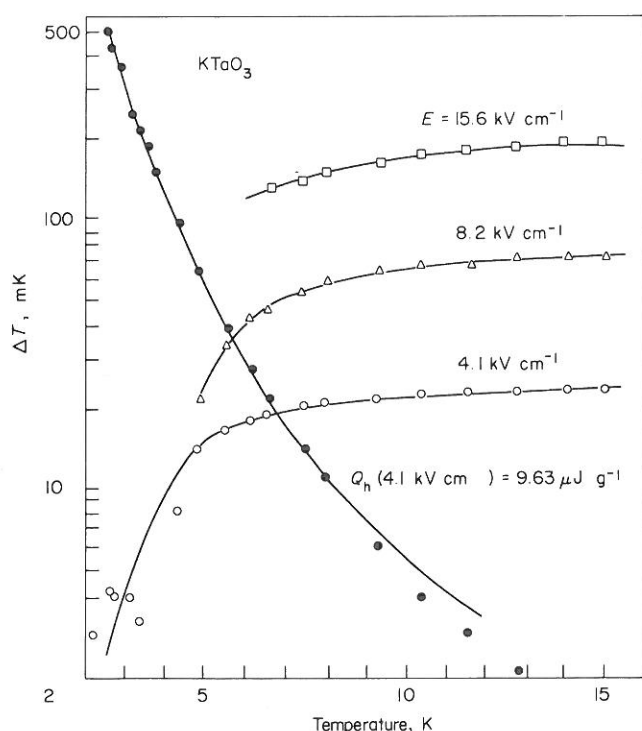


Fig. 10 Typical electrocaloric data measured on a KTaO₃ single crystal.⁵⁵ The open symbols represent the reversible component and the full symbols represent the irreversible component for 4.1 kV cm⁻¹. Note that at this field strength, no cooling effects are seen for $T \lesssim 7$ K

KTaO₃ Single crystal and ceramics

The dielectric constant of the single crystal sample showed a slight hump at about 3 K and decreased rapidly at temperatures above this. The hump was more pronounced in vanadium doped ceramic samples of KTaO₃. The polarization behaviour of the single crystal and ceramic samples were qualitatively the same as for SrTiO₃. Details of those measurements are given in a separate publication.⁵⁴ In general, the values for P_t and $\partial P_t/\partial T$ per unit field for the single crystal KTaO₃ were slightly less than that of the pure SrTiO₃ ceramics.

The electrocaloric effect⁵⁵ in single crystal KTaO₃ was in agreement with that expected from the polarization measurements. As shown in Fig. 10, the largest observed cooling effect was about 0.2 K at 10 K for a field of 15.6 kV cm⁻¹. For SrTiO₃ a similar field gave cooling of about 0.26 K, although the specific heat of SrTiO₃⁵³ is less than that of KTaO₃.⁵⁵ These specific heats will be discussed in more detail later.

Pb₂Nb₂O₇ ceramic

Previous measurements⁵⁶ of the dielectric constant of Pb₂Nb₂O₇ showed a peak at about 17 K which was attributed⁵⁶ to an antiferroelectric transition. Such a transition would mean that large electrocaloric effects may be possible. Thus measurements of polarization were made on a ceramic of this material to determine the magnitude of possible cooling effects. The results⁵⁷ for $\partial P_t/\partial T$ were considerably smaller than those for SrTiO₃ and KTaO₃. In addition the polarization appears to be constant in the 4-15 K region. As discussed by Siegwirth et al⁵⁷ the data suggest that no antiferroelectric transition takes place in Pb₂Nb₂O₇. Based on the polarization measurements, electrocaloric cooling effects were expected to be small and were not measured.

Polar ceramics

A well known series of polar ceramics is that of the PbZr_xTi_{1-x}O₃ (PZT) system. The system is ferroelectric at room temperature for $X \lesssim 93\%$, but for $X \gtrsim 93\%$ the system is antiferroelectric.⁵⁸ The antiferroelectric 95/5 PZT is interesting for this programme since hysteresis effects should be small. Polarization measurements at low temperatures had not been done previously. However, the high ordering temperature would suggest that $\partial P/\partial T$ is small at 4 K. Measurements of $P(T)$ below 77 K were made for both 65/35 PZT and 95/5 PZT with very similar results. Both showed negative $\partial P/\partial T$ values, but for the antiferroelectric 95/5 PZT one would expect the slope to be positive.

Electrocaloric measurements were made on the 95/5 PZT sample with depolarization resulting in cooling. Such an effect is consistent with the observed negative $\partial P/\partial T$. Fig. 11 shows the temperature dependence of the electrocaloric effects for a field of 13.9 kV cm⁻¹. The temperature changes are certainly too small to be of any practical use and hysteretic heating dominates the cooling effects below about 9 K. The specific heat of 95/5 PZT has been reported previously.⁴⁹

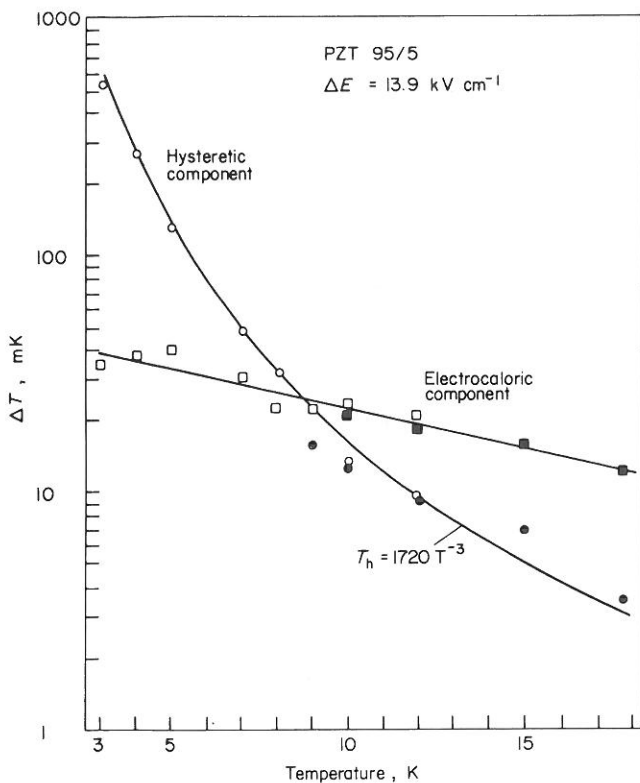


Fig. 11 Electrocaloric and hysteretic effects in 95/5 PZT as a function of temperature for a field change of 13.9 kV cm^{-1} .

TlBr and TlCl

The dielectric constant of TlBr, TlCl and TlI were measured by Samara⁵⁹ between 76 and 400 K. All three materials show very similar behaviour of the dielectric constant, which increases with a decrease in temperature. At 76 K and below values of $\partial K'/\partial T$ are of the order of -0.02 K^{-1} compared to about -80 K^{-1} for SrTiO_3 . Measurements on TlCl between 0.015 and 10 K showed that the dielectric constant levels off and becomes independent of temperature below about 3 K.⁶⁰ The dielectric constant of TlBr is expected to behave the same way in that temperature range. Such behaviour is typical for a material which remains paraelectric at all temperatures down to 0 K.

The electrocaloric effect in both TlCl and TlBr were undetectable. This was to be expected because of the small value of $\partial K'/\partial T$. The specific heat of each of these materials was measured between 2 and 20 K, and reported on previously.⁴⁹ The specific heat of TlBr will be discussed more in the following section.

Discussion

Several questions have been brought to light by the measurements in this programme. In this section we discuss and attempt to explain the following observations: (i) the lack of cooling in SrTiO_3 glass ceramics at 4 K; (ii) the agreement between polarization and electrocaloric measurements; (iii) the peak in the dielectric constant in most dielectrics at low temperatures; (iv) the reason for the remanent polarization in most dielectrics at low temperatures; and (v) the specific heat and its relation to electrocaloric refrigeration. We also try to predict the electrocaloric effect

in fields much higher than those used in the present study. The fields used here were limited by the breakdown strengths of the samples. Only the multilayer glass-ceramic samples had high breakdown strengths. Then, finally, we make some general conclusions regarding the low temperature behaviour of dielectrics and the potential of electrocaloric refrigeration.

Adiabatic polarization cooling of SrTiO_3 glass ceramics was predicted because of large positive values of $\partial K'/\partial T$ at 4 K. The polarization calculated from K' , assuming no remanent, would also have this positive slope. However, actual measurements of P on glass ceramics, ceramics, and single crystals not only showed the presence of hysteresis, but also no sign of a positive slope in $P(T)$ when the samples were cooled in a field. Electrocaloric measurements agreed well with those predicted from measured $P(T)$ data. What then gives rise to the peak in the dielectric constant and the remanent polarization? We address this question below.

Dielectric properties

Earlier measurements of the electrical properties of SrTiO_3 by Weaver⁶¹ have shown hysteresis in the P - E data up to 45 K. Burke and Pressley⁶² saw hysteresis in the P - E curves with stress applied, and attributed the hysteresis to surface charge build up. Saifi and Cross⁶³ have measured apparent antiferroelectric hysteresis loops in some cases. Earlier work on ceramic SrTiO_3 showed a peak in $K'(T)$ in one case but not in another.⁶⁴

Similar results have been obtained for KTaO_3 . A peak in $K'(T)$ was observed originally by Hulm et al.⁶⁵ Recent measurements by Demurov and Venetsev⁶⁶ have shown a peak at 10 K. Dielectric measurements in this laboratory on the single crystal of Samara and Morosin⁴⁶ showed a slight peak in $K'(T)$ at 3 K. Hysteresis loops have been observed in P - E curves up to 56 K on ceramic samples of KTaO_3 .⁶⁶

Until recently there existed no model of electrical behaviour for SrTiO_3 or KTaO_3 that explained hysteresis or peaks in $K'(T)$ without assuming a ferroelectric or an antiferroelectric transition. Siegwath and Morrow⁴⁷ have suggested a model which explains the behaviour of the dielectric constant and the polarization. This model considers permanent dipoles, due to impurities, that have a thermal electret state and which give rise to very low frequency dielectric relaxation effects. The model also explains the presence of apparent ferroelectric hysteresis curves without requiring an ordering transition. In essence that model is one of a thermoelectret formed from permanent dipoles. The strong dependence of the dielectric behaviour on impurities suggests permanent dipoles similar to the impurity-vacancy (I - V) dipole that has been studied extensively in alkali halides.⁶⁷⁻⁷⁰ In the materials studied here these dipoles are trapped at sufficiently low temperatures so they cannot freely rotate. This trapping may be a result of electric dipole-dipole interactions as suggested for the case of alkali halides.⁷¹ The dipoles can be aligned relatively easily when a field is applied at a high temperature (77 K). When the field is removed at 4 K, the dipole orientation is frozen in,

resulting in a remanent polarization. The dipoles gradually become randomly oriented as the sample temperature is increased. The total polarization of the sample is the sum of that due to these permanent dipoles and that due to the intrinsic lattice, such as SrTiO₃ or KTaO₃. It is emphasized that no long range order between dipoles need occur in a thermoelectret as does in a ferroelectric.

The thermoelectret model also explains the peaks in the dielectric constant. The presence of permanent dipoles from impurities means that they will contribute to the dielectric constant of the intrinsic material, but only when they are free to move at the frequency of the measuring field. At 0 K they would be completely frozen in and could not contribute to the dielectric constant. As the temperature is raised, it becomes easier for the dipoles to follow the alternating measuring field. The permanent dipole contribution to the dielectric constant starts off at zero at $T = 0$ and asymptotically approaches a maximum value as the temperature is increased. The intrinsic behaviour for the dielectric constant of the SrTiO₃ or KTaO₃ lattice is one of a constant value at very low temperatures ($T \lesssim 4$ K), but at higher temperatures it begins to drop and approach a T^{-1} dependence in accordance with Barrett's theory.²⁶ When the permanent dipole contribution is added to the intrinsic behaviour, the resultant dielectric constant has a peak at some temperature which depends on the impurity type and concentration. Further details of this thermoelectret model are given elsewhere.⁴⁷ Because the permanent dipoles are not free to move in the 4–15 K temperature range, they contribute little to the electrocaloric effect.

Thermal properties

For temperatures somewhat above 4 K, the term $\partial P/\partial T$ in most materials studied become reasonably large and negative, especially for SrTiO₃ and KTaO₃ (single crystal, ceramic or glass-ceramic). The largest $\partial P/\partial T$ values, hence largest entropy changes, occur in the 20–50 K temperature range. The observed adiabatic depolarization cooling in this temperature range agreed well with that predicted from the measured $\partial P/\partial T$ and specific heat via (3). The actual temperature changes were always less than 1 K for the field strengths used. It was uncertain how much further the temperature could be reduced by using much larger fields, since $\partial P/\partial T$ was not known at higher fields. If $\partial P/\partial T$ could be measured in sufficiently high fields to make $\partial P/\partial T$ approach zero, then the maximum entropy change could be calculated. Since all the materials studied had $\partial P/\partial T < 0$, an applied electric field always decreases the entropy. The maximum entropy change then would be just the value of the field dependent entropy of the material, or the dipolar entropy in zero field. When that is subtracted from the zero field entropy, the remainder is the intrinsic lattice entropy, which is field independent. As will be discussed later, the lattice entropy can be influenced slightly by an electric field in some cases. In those cases the maximum entropy change can be larger than the case where the lattice entropy is field independent. In any case the maximum entropy change can be no larger than the total entropy in zero field. Such a limit indicates the maximum refrigeration power

which can be expected from a material, even through the material could cool itself down from any temperature. In a paper on refrigeration fundamentals, Radebaugh⁷² shows that an entropy change of at least $\Delta S/R = 10^{-2}$ to 10^{-1} at 4 K is necessary for practical refrigeration. We have shown earlier that an electrocaloric refrigerator would require $\Delta S/R = 10^{-2}$ for practical refrigeration in most cases.

At this point we are faced with the problem of determining the total zero field entropy and then separating that into the dipolar and lattice contributions. Equation (9) can be used to determine the total zero field entropy if the specific heat is measured to a sufficiently low temperature. For low enough temperatures, $\partial P/\partial T = 0$ and $\partial^2 P/\partial T^2 = 0$, and the dipolar contribution to the specific heat should be negligible. According to (5) the specific heat is independent of field in that temperature region. For all the materials studied in this programme, 2 K was a sufficiently low temperature to insure $\partial P/\partial T$ and $\partial^2 P/\partial T^2$ were negligible. Specific heat results on these samples showed that C/T^3 was beginning to level off in the range below about 2–4 K and approach the value predicted by elastic constants. For some of the materials, such as SrTiO₃ and KTaO₃, it would be desirable to have specific heat measurements down to 1 K or below to accurately extrapolate C/T^3 to 0 K. However, because $C \propto T^3$, the temperature range below 1 K contributes only about 2% to the entropy at 4 K. Considerable uncertainties in C/T^3 below 1–2 K are then of little consequence.

The only cause for concern in extrapolating the specific heat to 0 K is that an anomaly in the specific heat may be present in that temperature interval. Only an anomaly which is influenced by an electric field is of any consequence since any other type would simply shift all the curves in Fig. 1 by the same amount. From a theoretical standpoint, there is no reason to expect any such anomaly in the range below 1 K.

Separation of the total entropy into the lattice and dipolar parts could be done experimentally if a sharp transition occurred. The lattice part would be the background entropy. This separation is commonly done for materials with ferroelectric transitions near room temperature.⁶⁴ When the dipolar entropy is small and there are no sharp transitions, it becomes difficult to separate the two from experimental specific heat results. Such is the case with all the materials studied in this programme. To help in the separation, we have made use of theoretical models. Ferroelectric and antiferroelectric transitions are usually classified into order-disorder or displacive type transitions.^{64, 73} For order-disorder materials a permanent dipole moment exists even in the non-polar phase which implies the existence of a double potential well for the ion or group of ions. This kind of dielectric material is very much analogous to magnetic substances. The other class of dielectric transitions is the displacive type. In these materials the potential well, $V(X)$, has only one minimum and is slightly anharmonic. A permanent dipole moment does not exist in these materials above the transition temperature, but the application of an electric field induces a moment. The thermal properties of these two classes of dielectrics can be quite different and so we consider each class separately.

Displacive materials. As the temperature is lowered in these materials, the long and short range forces on the ion can change in such a way that they tend to cancel each other at some temperature. When this occurs, $\partial^2 V/\partial X^2 = 0$ at $X = 0$ and the ion becomes unstable at the position $X = 0$. A small displacement of the ion can occur at and below that temperature and the material becomes a displacive ferroelectric or antiferroelectric. A lattice dynamic description of such materials, as introduced by Cochran,⁷⁴ and Anderson⁷⁵ has proven very useful.⁷³ In this description the frequency, ω , of the optic phonon mode decreases as the temperature is lowered. At the transition temperature ω becomes zero at some value of the wave number q . The process is called a condensation of a soft mode. If the condensation occurs at $q = 0$, the transition is to the ferroelectric state, whereas if it occurs at the Brillouin zone boundary, an antiferroelectric transition occurs. An electric field has a strong effect on the soft mode.

The ABO_3 compounds having the perovskite structure usually display the displacive type transitions. The material $PbTiO_3$ is the most ideal example in the sense that the soft optic mode is sharp and underdamped in contrast to $BaTiO_3$ where the soft optic mode is highly over-damped.⁷⁶ Both $SrTiO_3$ and $KTaO_3$ are good examples of displacive or soft optic materials though the optic mode never quite condenses at $q = 0$ even for $T = 0$ K. These materials could be called incipient ferroelectrics. All of the materials studied in this programme are probably of the displacive type, since the order-disorder type did not show strong dielectric activity in the 4–15 K temperature range.

The lattice dynamic description of the displacive materials provides a simple way of separating the lattice and dipolar entropies. In such a model the lattice entropy is that associated with the acoustic modes and the dipolar entropy is that of the optic modes. Recent neutron scattering experiments using high flux reactors have been valuable for mapping out the phonon dispersion curves of several of the materials studied in this programme. Various thermodynamic properties of the material can then be calculated from these phonon dispersion curves. For instance, when the phonon dispersion curves are independent of the temperature, the specific heat is given as⁷⁷

$$C = \frac{Vk}{8\pi^3} \sum_p \iiint \frac{x^2 \exp(x)}{(\exp(x) - 1)^2} dq^3, \quad (11)$$

where V is the volume, k is Boltzmann's constant, q is the wave number, p refers to summation over all polarizations, and x is given by

$$x(q, T) = \hbar\omega(q)/kT. \quad (12)$$

The summation over the polarizations refers to the various transverse and longitudinal modes in the acoustic and optic branches. The transverse modes are doubly degenerate in both the acoustic and optic branches. In general, the phonon dispersion curves have not been measured in enough directions or in enough detail to warrant solving (11) exactly. Instead we make the assumption that the phonon dispersion curves are the same in all directions and approximate the Brillouin zone with a sphere. With those approximations

we get

$$\frac{C}{3R} = \sum_p \int_0^1 \frac{x^2 \exp(x)}{(\exp(x) - 1)^2} y^2 dy, \quad (13)$$

where $y = q/q_{\max}$. For a cubic crystal with a zone boundary of $q_{B,Z}$ along a [100] direction, q_{\max} for the spherical approximation is

$$q_{\max} = (6/\pi)^{1/3} q_{B,Z}. \quad (14)$$

With these approximations the entropy is given by

$$\frac{S}{3R} = \sum_p \int_0^1 \left[\frac{x}{\exp(x) - 1} - \ln(1 - \exp(x)) \right] y^2 dy. \quad (15)$$

If the dispersion curves are functions of temperature, (15) is still valid for the entropy,⁷⁸ but then the specific heat must be calculated from

$$C = T\partial S/\partial T. \quad (16)$$

The materials studied in this programme had phonon dispersion curves that were nearly temperature independent below 15 K. Thus, (13) and (15) were used in all the calculations since the region of main interest in this programme is that below 15 K. The calculations for C and S were carried out to 40 K and, in general, the error introduced in C at that temperature by not using the exact technique of (16) is probably the order of 10%. That uncertainty is still smaller than the possible error introduced from the uncertainty in the phonon dispersion curves.

Fig. 12 shows the phonon dispersion curves for $SrTiO_3$ used for the thermodynamic calculations. For low q , the curves are based on the neutron scattering work of Yamada and Shirane.⁷⁹ The slopes of the acoustic modes at $q = 0$ are consistent with the elastic constant measurements of Bell and Rupprecht.⁸⁰ The Debye temperature, normalized to one atom per molecule, derived from the elastic constants is 390 K. The double valued part of the transverse optic (TO) curve at low q and $E = 0$ indicates the uncertainty of the curve. The upper curve is based on the neutron work⁷⁹ and the lower curve is based on induced Raman scattering work.⁸¹ The difference is outside experimental error and has been attributed to thermal aging which causes an increase in the energy with time. The lower curve was used in our calculations because it is more consistent with that derived from dielectric constants using the Lyddana-Sachs-Teller relation,

$$K'_0/K'_\infty = \omega_{LO}^2/\omega_{TO}^2, \quad (17)$$

where K'_0 and K'_∞ are the static and high frequency dielectric constants, ω_{LO} and ω_{TO} refer to the longitudinal and transverse optical phonon frequencies. In any case, the total entropy or specific heat would be reduced by less than 1% if the upper curve was used. The TO mode dispersion curves for various values of electric field are estimates based on the $q = 0$ values from Raman scattering data.⁸¹

There are no measurements of the field dependence of the TA mode although Bell and Rupprecht⁸⁰ find a very slight softening of the elastic constants for fields up to about 20 kV cm⁻¹. If there is an interaction between the TO and TA modes, then it is reasonable to expect that the soft

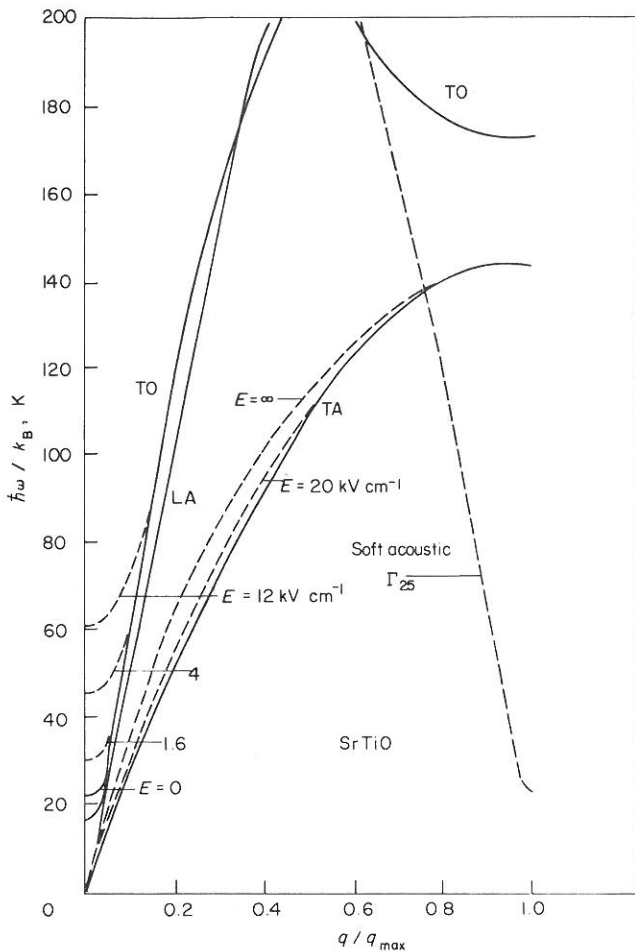


Fig. 12 Phonon dispersion curves for SrTiO₃ used for thermodynamic calculations. The curves are based on neutron and Raman scattering work

TO mode forces a softening in the TA mode. Thus, lifting the TO mode with an electric field can result in a lifting of the TA mode. An estimate of the effect of a field on the TA mode was made from the dispersion curves measured by Yamada and Shirane.⁷⁹ They found that the TA mode softened somewhat as the temperature decreased. First we assume that all of this change is caused by the lowering of the TO mode rather than an intrinsic temperature effect. Then we can say that when an electric field lifts the TO mode, the TA mode is also lifted. The behaviour of the TA mode below 15 K in an electric field is then taken to be the same as in zero field, but at a temperature corresponding to the case where the TO mode in zero field has risen to the value it would have in an electric field at low temperature. According to this argument we use the behaviour of the TA mode at 120 K in zero field as the behaviour for low temperatures and 20 kV cm⁻¹. For $E = \infty$ we use the behaviour at $T = 300$ K, since the TO mode at that temperature is so high above the TA mode that no more interaction occurs. Thus, lifting the TO mode higher by an electric field would have no further effect on the TA mode. Fig. 12 shows these estimates for the TA mode in fields of 20 kV cm⁻¹ and infinity. Because there may still be some intrinsic temperature effect on the TA mode, these estimates represent upper limits for those fields.

For high values of q , the dispersion curves in Fig. 12 are based on the work of Shirane and Yamada⁸² and of Cowley.⁸³ The dashed line in Fig. 12 shows the soft acoustic mode, Γ_{25} , along the [111] direction which is responsible for the antiferrodistortive structural transition at 105 K. The curve as drawn is the position of the mode below about 40 K. The highly anisotropic nature of the Γ_{25} mode means that its contribution to the specific heat and entropy cannot be calculated by (13) and (15) since they assume an isotropic mode. Its contribution, however, is probably small and so a crude estimate was made. This was done by using (13) and (15) and multiplying the resultant C and S by a constant factor to give reasonable agreement with experiment. The factor used here turned out to be 10^{-2} .

Fig. 13 shows the calculated specific heat curves for SrTiO₃, plotted as C/RT^3 to remove most of the temperature dependence. The lower dashed curve for $E = 0$ is the contribution from the three acoustic modes. The middle dashed curve is the specific heat after adding on the contribution from the soft Γ_{25} mode. The top dashed line is the specific heat after the addition of the contribution from the doubly degenerate soft TO mode for $E = 0$. Also shown in the figure are experimental results for the specific heat of various SrTiO₃ samples. The polycrystal results are from two separate measurements^{84, 85} and the single crystal results are from the unpublished data of Colwell.⁵⁰ The specific heat of pure SrTiO₃ ceramic and the ceramic with 10% V are from this work although further details of the pure ceramic work have been published elsewhere.⁵³ For the cases of the single crystal and the polycrystal, agreement between experiment and theory is reasonably good. The elastic constants were measured above the 105 K transition and may not be correct for the low temperatures considered here. The specific heat of pure SrTiO₃ ceramic and SrTiO₃ ceramic with 10% vanadium agree with the calculated curve at the higher temperatures, but at lower

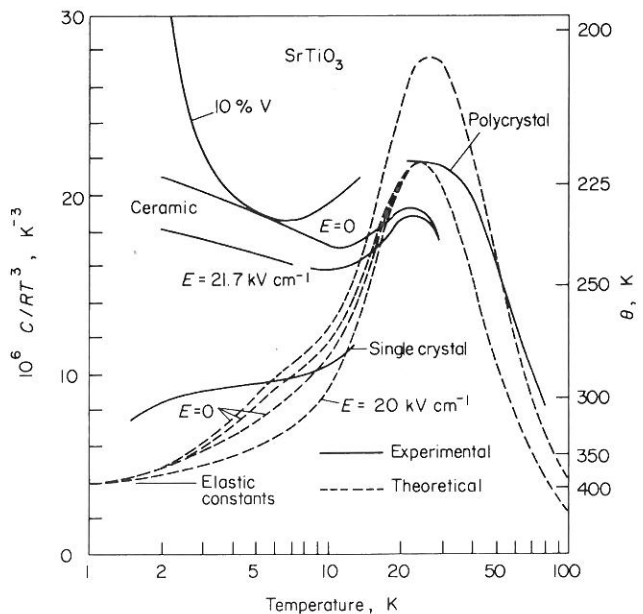


Fig. 13 Specific heat of SrTiO₃ calculated from the phonon dispersion curves as compared with experimental measurements. See text for explanation of the three theoretical curves

temperatures the deviation is considerable. The behaviour of the 10% V sample suggests that the rise in C/T^3 for low temperatures could be a result of impurities. Magnetic impurities could cause such a rise, or if the impurities result in electric dipoles, such as impurity-vacancy dipoles discussed earlier, then the impurity specific heat could contribute a $T^{3/2}$ term as seen in the doped alkali halides if the concentration is high enough.^{71, 86} The specific heat of the high purity SrTiO₃ ceramic does indeed have a $T^{3/2}$ behaviour.^{45, 53} A surface layer contribution has also been proposed⁴⁵ to account for the $T^{3/2}$ term.

An electric field of 21.7 kV cm⁻¹ lowers the specific heat of pure SrTiO₃ ceramic as shown in Fig. 13. The change is about 12% at 4 K. From a theoretical standpoint some reduction of the specific heat is expected. The electric field increases the TO mode as shown in Fig. 12 and so for temperatures below about 10 K the TO mode can no longer contribute to the specific heat for high fields. Thus, the theoretical specific heat in a field of 21.7 kV cm⁻¹ would be that shown by the middle dashed curve in Fig. 13 for temperatures below about 10 K. Experimentally, the reduction in the specific heat with an electric field is greater than that expected theoretically. The difference may be a result of a shift in the TA mode with electric field. When the estimated shift of a TA mode with an electric field of 20 kV cm⁻¹ is included in the theoretical model, the specific heat due to the acoustic modes is shifted to the lower dashed line in Fig. 13. The total change in the theoretical specific heat is then about the same as that observed experimentally, except for temperatures below about 4 K. The larger observed change below 4 K may be a result of impurity effects.

The phonon dispersion curves for KTaO₃ have been measured by Shirane et al.⁸⁷ and Axe et al.⁸⁸ The curves shown in Fig. 14 are based on their work. Since their work was primarily in the [100] direction, the curves shown in Fig. 14 may not represent the entire crystal. The slopes of the LA and TA modes are consistent with elastic constant measurements made at 2 K⁸⁹ and give a Debye temperature, normalized to one atom per molecule, of 327 K. A slight flattening of the TA mode occurs around $q/q_{\max} = 0.2$, which has been attributed to an interaction between the TO and TA modes.⁸⁸ The value of the TO mode at $q = 0$ in a field of 15 kV cm⁻¹ is based on induced Raman scattering data.⁸¹ The behaviour of the mode for higher q values with $E = 15$ kV cm⁻¹ is estimated. The electric field dependence of the TA mode is estimated by the same method used for SrTiO₃. Because of a rather strong TO-TA mode interaction in KTaO₃ an electric field has a greater effect on the TA mode of KTaO₃ than on SrTiO₃. To account for the considerable anisotropy of the interaction,⁸⁸ we allow one of the TA modes to remain independent of field for our calculations.

Fig. 15 shows the calculated specific heat of KTaO₃ in comparison with the measured values. The theoretical curve for $E = 15$ kV cm⁻¹ is lower than the $E = 0$ curve because of the TA mode hardening. The TO mode contributes a small amount to the $E = 0$ curve for temperatures above 30 K as shown by the splitting of that curve on the upper end. Thus an electric field effect due to the TO mode would occur

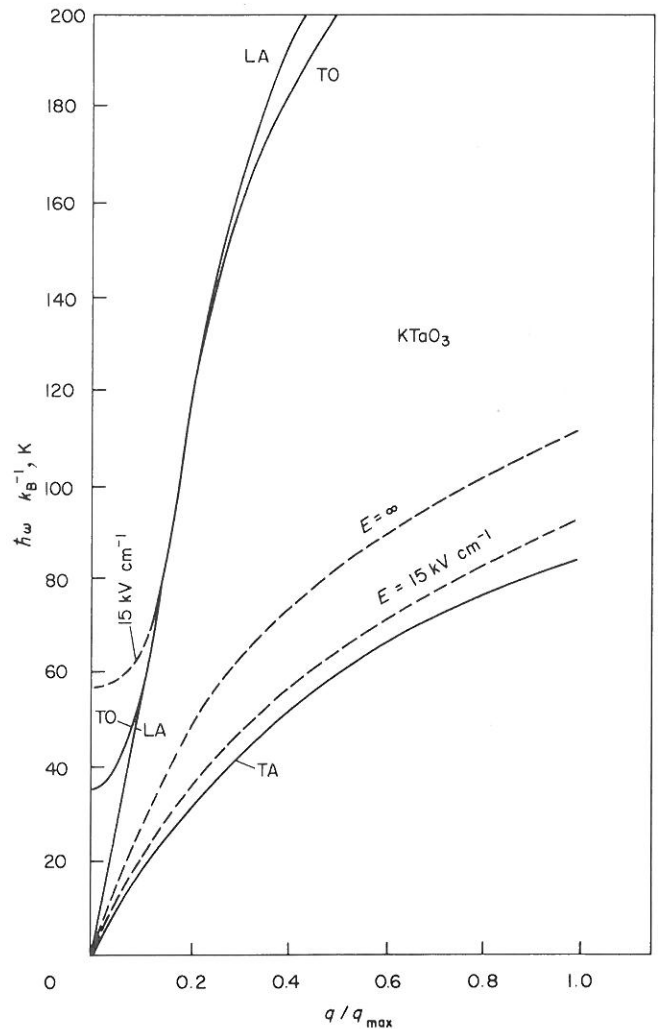


Fig. 14 Phonon dispersion curves for KTaO₃ used for thermodynamic calculations. The curves are based on neutron and Raman scattering work

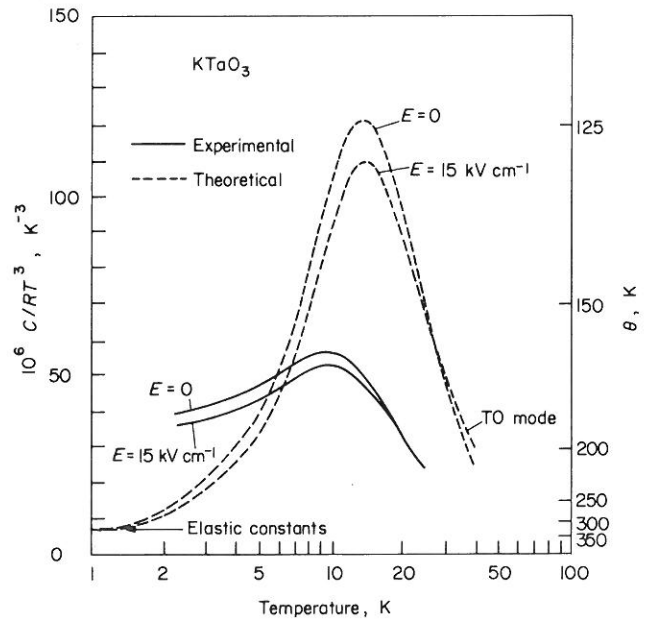


Fig. 15 Specific heat of KTaO₃ calculated from the phonon dispersion curves as compared with experimental measurements. The calculated TO mode contribution is significant only at the highest temperatures

only above 30 K. The discrepancy between the experimental and theoretical curves at high temperatures could be explained by uncertainties in the behaviour of the TA dispersion curve over all directions. The neutron measurements were made only along the [100] direction. Impurities may account for the disagreement between the measured specific heat at low temperatures and that expected from the elastic constants and the measured dispersion curves. The observed change in specific heat with an electric field of 15 kV cm^{-1} agrees well with the calculated shift.

A material studied in this programme which showed no cooling effects was TlBr. For the sake of comparison we also have calculated the thermodynamic properties of this material. The phonon dispersion curves used in these calculations⁴⁴ are based on the neutron scattering work of Cowley and Okazaki.⁹⁰ The TA mode is fairly anisotropic with the (0, 0, 1) direction giving the lowest values and the (1, 1, 1) direction the highest. Thus, instead of considering the TA mode doubly degenerate as for SrTiO₃ and KTaO₃, these two curves were used in the thermodynamic calculations. Such a process tends to average the two curves. The acoustic modes are consistent with a Debye temperature, normalized to one atom per molecule, of 100 K. Elastic constant measurements yield a Debye temperature of 105 K,⁹¹ normalized to one atom per molecule. The TO mode is quite high ($\hbar\omega/k_B = 62 \text{ K}$ at $q = 0$) and independent of temperature; thus it would not be considered a soft mode. The dielectric constant obeys a Curie-Weiss law, but the temperature dependence is a result of anharmonic lattice effects rather than a softening of the TO mode.⁵⁹ The material is paraelectric for all temperatures and never even approaches a ferroelectric transition as do SrTiO₃ and KTaO₃.

The calculated specific heat of TlBr is shown in Fig. 16 and compared with the experimental curve. There is excellent agreement between the two curves. This material has a rather large specific heat which is a result of the low-lying acoustic modes. As shown by the upper dashed line, the TO mode contributes little to the total specific heat.

Theoretical calculations for the thermodynamic properties of PZT and P₂Nb₂O₇ cannot be done since there have been no measurements of the phonon dispersion curves. The three specific heat comparisons (SrTiO₃, KTaO₃, and TlBr) between theory and experiment indicate that the lattice dynamic model gives a reasonably good description of the thermodynamic properties of the displacive type materials. In all three cases, however, the TO mode contributed only a small part of the total specific heat. Thus the specific heat measurements are not a very sensitive measure of the thermodynamic properties associated with the TO mode.

The TO mode contribution could be factors of 2-5 higher before the agreement with experiment is deteriorated significantly. Nevertheless, because of the good agreement in the total specific heat, we shall proceed with the assumption that both the acoustic and TO mode contributions to the thermodynamic properties are well described by the lattice dynamic model.

With the lattice dynamic model, we now have the means for separating the dipolar and lattice entropies for the displacive

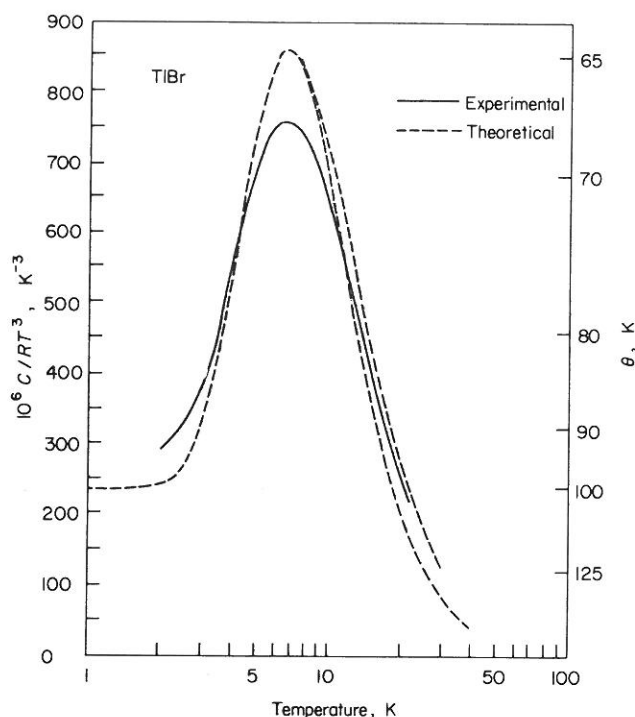


Fig. 16 Specific heat of TlBr calculated from the phonon dispersion curves as compared with experimental measurements

type materials. The soft transverse optic (TO) mode is in general strongly temperature dependent and is responsible for the polarization of the material. Initially we assign the dipolar entropy as that associated with the soft TO mode and the lattice entropy as that of the acoustic mode. Electric fields have a strong effect on the static dielectric constant and by the LST relation in (17) they also have a strong effect on the frequency of the soft TO mode. An applied electric field has the effect of hardening the TO mode, ie increasing the frequency of the mode. The effect is greatest for that part of the Brillouin zone in which the TO mode has the lowest frequency. This is the zone centre for ferroelectric type materials and the zone edge for anti-ferroelectric type materials. At the other extreme of the zone, the electric field should have little effect on the TO mode. The materials studied here are of the ferroelectric type so that an electric field increases the frequency at the zone centre, but has little effect on the frequency at the zone edge. We then expect that as the electric field increases to infinity, the soft TO mode hardens and becomes nearly constant for all wave numbers. This constant value is just that of the original soft mode at the zone edge. These two extreme positions for the TO mode then can be used for the dipolar entropies at $E = 0$ and $E = \infty$. As discussed earlier, the electric field can affect the TA modes via the TO-TA mode interaction when the TO mode energy approaches that of the TA mode. In those cases the TA mode can contribute to the dipolar entropy. Estimates of the behaviour of the TA mode in electric fields were made for SrTiO₃ and KTaO₃.

Fig. 17 shows the entropy of the acoustic and optic modes calculated via (15) for SrTiO₃. For $E = \infty$ we have taken the value $\hbar\omega/k = 185 \text{ K}$ for the TO mode, which tends to level

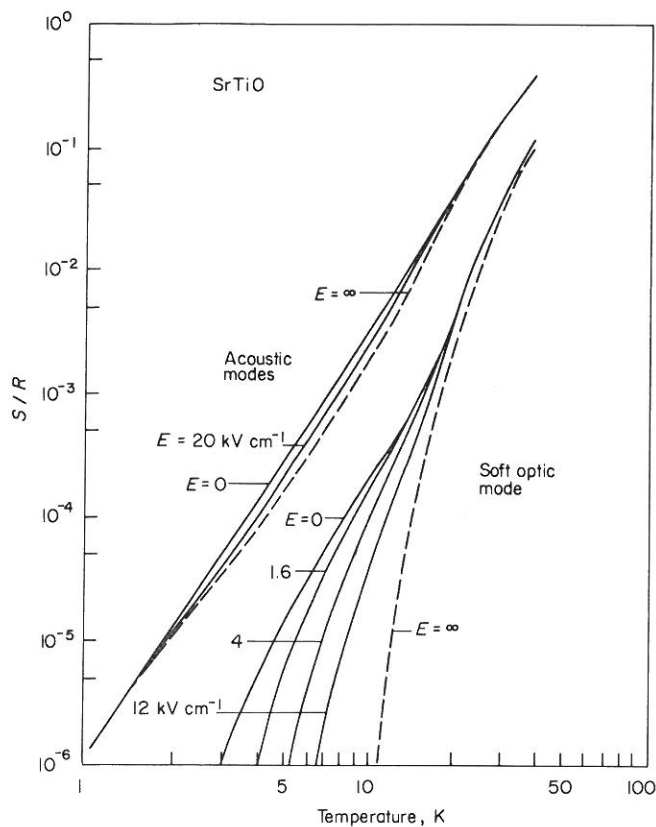


Fig. 17 Entropy of the acoustic and optic modes of SrTiO₃ calculated from the phonon dispersion curves

out the hump in that mode. The calculated entropy for that case is just two-thirds the Einstein entropy of a material with an Einstein temperature of 185 K. The difference between the $E = 0$ and $E = \infty$ curves gives the maximum entropy change possible. For SrTiO₃ the acoustic mode may contribute a large fraction of the entropy change with field. We recall that it was desirable to have entropy changes of the order of $\Delta S/R \approx 10^{-2}$ at 4 K for a practical refrigerator. As shown in Fig. 17, the maximum optic mode entropy change is over three orders of magnitude less than the desired amount, but the change in the acoustic mode is about two orders of magnitude less. Since temperature changes during adiabatic depolarization would be expected to be small, we calculate these changes by

$$\frac{\Delta T}{T} = \frac{\Delta S}{T(\partial S/\partial T)} = \frac{\Delta S}{C} \quad (18)$$

where C is the total specific heat of the material in zero electric field. For the case where $\Delta T/T$ is not much smaller than one, the temperature change must be determined from isentropic lines in a plot of S vs T .

Fig. 18 shows the calculated temperature changes in SrTiO₃ when depolarizing from various E values. The lower set of curves is for the case where the electric field influences only the TO mode, whereas the upper two curves take into account the estimated contribution from the TA mode as well. For $E = \infty$ the calculated curve for the TA + TO modes peaks at about $\Delta T/T = 0.15$ at 9 K and drops to 0.09 at 4 K. This curve is not shown in Fig. 18. Shown for comparison in Fig. 18 are some experimental measurements. The work of Kikuchi and Sawaguchi²⁸ was for 7 kV cm⁻¹ on a single crystal and

that of Hegenbarth²⁹ was for a field of 10 kV cm⁻¹ on a single crystal. Hegenbarth's original work²⁷ on a ceramic sample in a field of 8 kV cm⁻¹ above 17.5 K gave results nearly equal to that of the present work for a field of 5.4 kV cm⁻¹. The present work was also on a ceramic sample but, unlike Hegenbarth's results, the present results show only the reversible electrocaloric effect. Nevertheless the present results on a high quality ceramic sample are not quite as good as those of Kikuchi and Sawaguchi on a single crystal for the same value of electric field. This is to be expected since the electric field in a ceramic may be concentrated at grain boundaries rather than in the bulk SrTiO₃.

In comparing theory and experiment we concentrate especially on the single crystal work of Kikuchi and Sawaguchi since that appears to be the most ideal sample. It is obvious from Fig. 18 that the observed temperature changes are greater than that expected if only the TO mode is considered. Thus interactions between the TO mode and the TA mode must be present to account for the observed ΔT . When this interaction is considered, the theoretical ΔT for 7 kV cm⁻¹ is in reasonable agreement with the single crystal work of Kikuchi and Sawaguchi. It is emphasized here that the theoretical results for ΔT which include the TA mode contribution are based on rough estimates of the effect of a field on the TA mode. Thus the good agreement with experiment may be fortuitous. The theoretical curves show that it may be possible to produce a cooling effect of about 1 K at 10 K for very high fields in SrTiO₃. However, such cooling effects are still too small to be of any practical use in most situations.

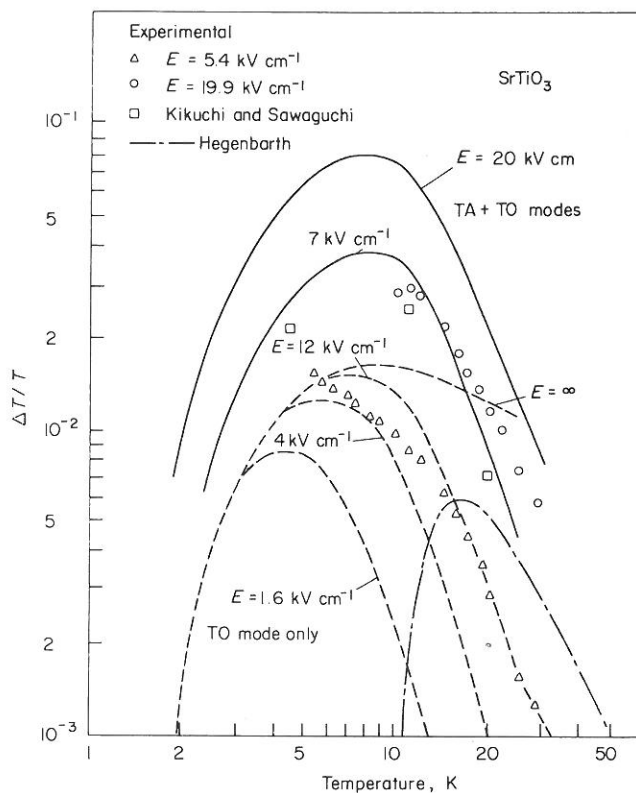


Fig. 18 Calculated temperature changes in SrTiO₃ during depolarization as compared with experimental results

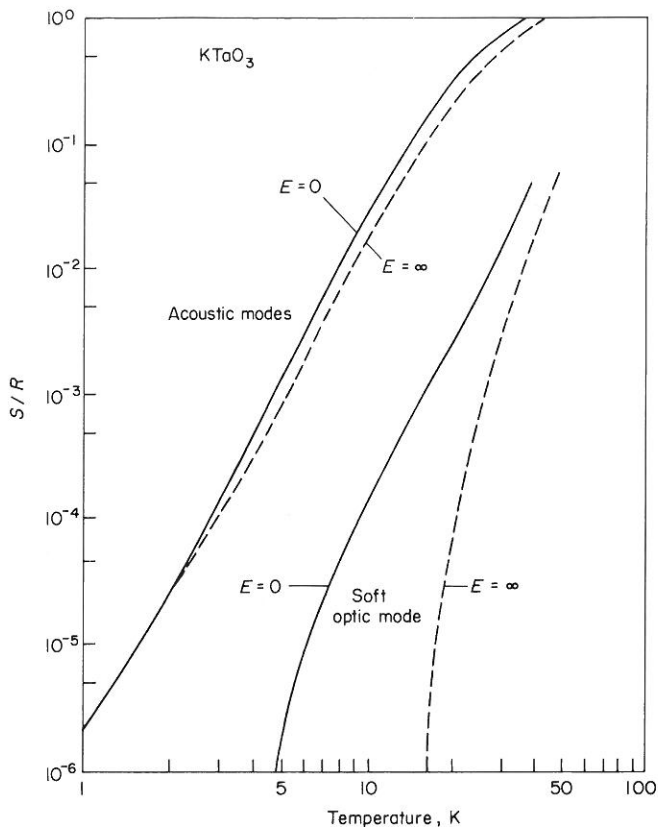


Fig. 19 Entropy of the acoustic and optic modes of KTaO_3 calculated from the phonon dispersion curves

Fig. 19 shows the calculated optic and acoustic mode entropies for KTaO_3 . The soft optic mode entropy is less than that for SrTiO_3 , whereas the acoustic mode entropy is higher than that of SrTiO_3 . The entropies at 4 K are much less than the desired value of $S/R = 10^{-2}$. Calculated electrocaloric temperature changes for different initial fields and zero final field are shown in Fig. 20. Experimental results on a KTaO_3 single crystal with a depolarizing field of 15.6 kV cm^{-1} are shown for comparison. Both the experimental results and the calculated curve are less than for SrTiO_3 , except for the calculated curves above 15 K. The experimental values for $\Delta T/T$ are in reasonable agreement with calculated values in view of the uncertainty of the phonon dispersion curves.

The entropies of the acoustic and TO modes for TlBr were calculated but are not shown here. The TO mode for TlBr , unlike SrTiO_3 and KTaO_3 , does not soften at the zone centre, i.e. the phonon frequency is nearly independent of wave number. Thus an electric field should have little effect on the TO mode and its entropy, as was evident by the calculated entropy curves. The entropy of the acoustic mode is of the order of $S/R = 10^{-2}$ at 4 K, but little interaction would be expected between the TO and acoustic modes because of the large difference in energy between the two modes. Thus, the electric field should have little effect on the acoustic mode. Theoretically the temperature changes during adiabatic depolarization are very small (about 1 mK at 7 K) and probably not observable. As expected, no temperature changes could be detected experimentally (resolution of a few mK).

Except for PZT, none of the displacive type materials showed a transition to the ferroelectric or antiferroelectric state. Instead they remained incipient ferroelectrics down to 0 K. If a displacive transition to the ferroelectric state did occur at a low temperature, would the dipolar entropy then be high enough for a practical refrigerator? To answer this question we look at the general behaviour of the soft TO mode dispersion curve. For the TO mode we consider a fairly simple, but reasonable⁹² dispersion curve of the form

$$\omega^2(q) = \Delta_0^2 + S^2 q^2, \quad (19)$$

where Δ_0 is the phonon frequency at $q = 0$ and S is a constant. Putting this equation in temperature units and in units of $y = q/q_{\text{max}}$ gives

$$\hbar\omega/k = [(\hbar\Delta_0/k)^2 + (cy)^2]^{1/2}. \quad (20)$$

Condensation of the TO mode would follow the behaviour of (20) as Δ_0 approaches zero. The condensation of the mode, which gives rise to a ferroelectric transition, can occur at any temperature.

Fig. 21 shows the entropy of the TO mode, calculated via (15), at various temperatures as a function of $\hbar\Delta_0/k$ for the case of $\hbar\omega/k = 200 \text{ K}$ at $y = 1$. From these curves we note that the TO mode entropy at the transition ($\Delta_0 = 0$) increases with temperature. Whereas S/R is significantly greater than 10^{-2} for a transition at 50 K, it is significantly less than 10^{-2} for a transition at 5 K. In SrTiO_3 a transition does not occur and instead $\hbar\Delta_0/k$ decreases to only 16 K. At 5 K the TO mode entropy for this case as shown in Fig. 21 is about $3 \times 10^{-4} R$. If the transition did occur, the entropy is increased by only a factor of three as seen in Fig. 21. Thus a transition in SrTiO_3 to the ferroelectric state would not

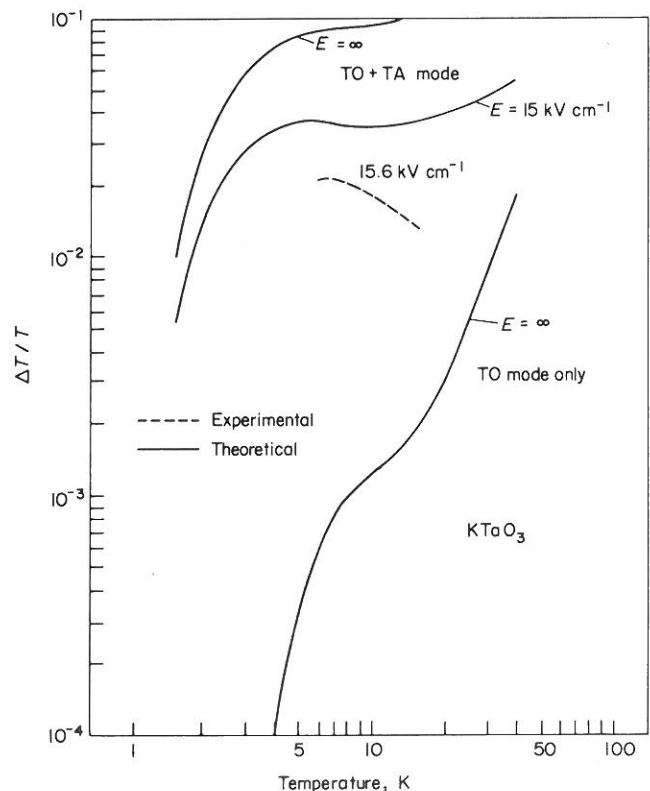


Fig. 20 Calculated temperature changes in KTaO_3 during depolarization as compared with experimental results

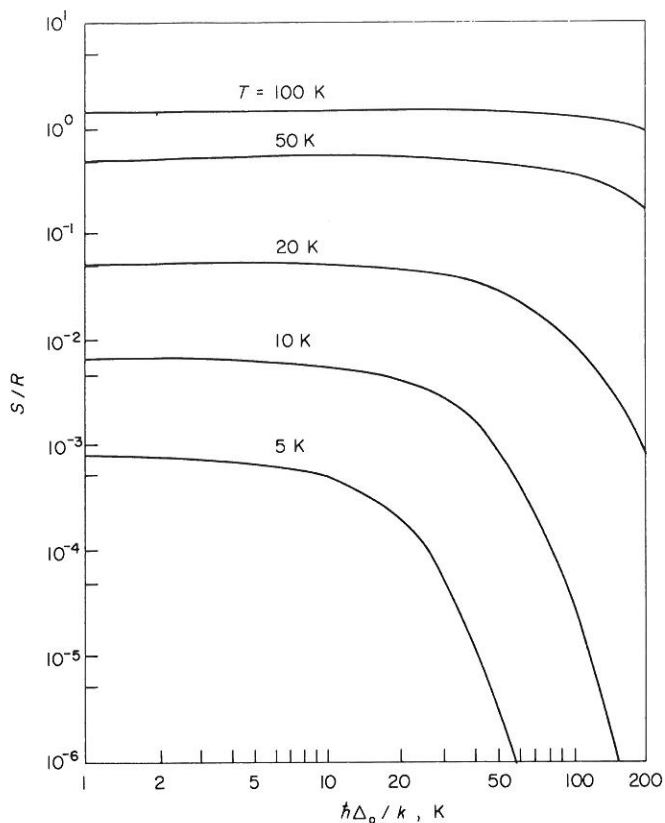


Fig. 21 Calculated entropy of the transverse optic mode from phonon dispersion curves of (10) as a function of $h \Delta_0/k$ for various temperatures

significantly increase the TO mode entropy. The maximum entropy change caused by a change in field from $E = 0$ to $E = \infty$ is the entropy at $h \Delta_0/k = 0$ minus the entropy at $h \Delta_0/k = 200$ K. The curve marked displacive in Fig. 22 shows this maximum entropy change as a function of temperature. The significance of the curve is apparent when it is compared with the minimum $\Delta S/R$ for practical refrigeration,⁷² also shown in Fig. 22. The displacive curve in Fig. 22 neglects any TA mode contribution that arise from TO-TA mode interactions. As shown for the case of SrTiO_3 and KTaO_3 , the TA mode contribution to the entropy change can dominate that from the TO mode. However, when the TO mode condenses (the case considered for the curve in Fig. 22) the TO mode entropy contribution is nearly comparable to that of the TA mode. Thus the effect of a strong TO-TA mode interaction would be to approximately double the entropy change from that shown in Fig. 22. In a material with a large TO-TA mode interaction the Debye temperature would have to be less than about 80 K (normalized to one atom per molecule) to provide enough lattice entropy for practical refrigeration at 4 K. No such material is known to exist. The displacive type materials can have enough entropy for practical refrigeration above 10 K, but then higher fields are needed to bring about the entropy change.

Order-disorder materials. In these materials a double potential well for the ion or group of ions exists even at temperatures above the transition temperature. These materials are well described by the use of pseudo-spin operators and so the thermodynamic behaviour of these materials is analogous to magnetic materials. Thus

depolarization cooling with an order-disorder dielectric should be completely analogous to adiabatic demagnetization of a paramagnetic material. In paramagnetic materials with total angular momentum of j there are $2j + 1$ possible orientations of the magnetic moment and so the entropy in the disordered state is $S = R \ln(2j + 1)$. For a dielectric material with two minimums in the single particle potential well, spin 1/2 operators are used in the description. Because of the two equilibrium positions of the particle in the disordered state, the dipolar entropy is $S = R \ln 2$ in the disordered state. Sufficiently high electric fields can order the dipole moments and so maximum entropy changes of the order of $R \ln 2$ are possible with order-disorder dielectrics above the transition temperature. As shown in Fig. 22, this entropy change is possible even at 4 K and below. Thus only these materials offer some probability for practical electrocaloric refrigeration at 4 K.

There are a few materials such as potassium dihydrogen phosphate and tri-glycine sulphate which are typically order-disorder type ferroelectrics. Specific heat measurements do indeed show entropy changes of the order of $R \ln 2$ at the transition from the ferroelectric to the paraelectric state. The transitions, however, occur at much too high a temperature to be useful for refrigeration at 4 K. The lowest transition temperature for a known order-disorder ferroelectric is 96 K for KH_2AsO_4 ⁷³ and 122 K for KH_2PO_4 .⁷³ The theoretical entropy and spontaneous polarization of such materials were derived by Devonshire.⁹³ According to that calculation S/R falls below 10^{-2} for $T/T_c < 0.3$ and continues to drop exponentially. Thus for KH_2AsO_4 below about 30 K the dipolar entropy is too small to make a useful refrigerator. In order to meet the

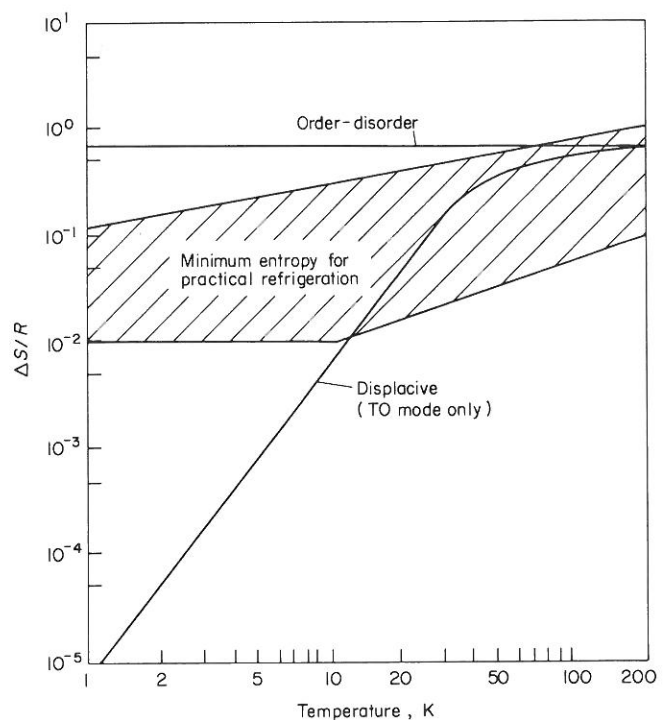


Fig. 22 Calculated maximum entropy change for a field change from E to ∞ to $E = 0$ in a model displacive material in which the TO modes has condensed at the zone centre. Shown for comparison are the maximum entropy change expected in an order-disorder material and the minimum $\Delta S/R$ needed for practical refrigeration

requirement of $S/R \gtrsim 10^{-2}$ at 4 K, it would be necessary to have an order-disorder material with a transition lower than about 13 K. If the ordered state is ferroelectric, then there still would be the problem of hysteretic heating during field changes.

The material lithium thallium tartrate ($\text{LiTlC}_4\text{H}_4\text{O}_6 \cdot \text{H}_2\text{O}$), hereafter abbreviated as LTT, has shown indications of a ferroelectric transition at about 11 K.⁹⁴⁻⁹⁷ A fairly pronounced peak in the dielectric constant occurs at 11 K for semi-transparent electrodes as well as a rapid softening of the lattice.⁹⁶ Both the elastic compliance and dielectric constant are strong functions of electric field in the region around 11 K. The structural similarity to Rochelle salt indicates it may be an order-disorder ferroelectric. Unfortunately there was not time to measure the specific heat and electrocaloric effects of this material because of the difficulties in obtaining a sample. Existing measurements⁹⁷ of the spontaneous polarization P_s can be used to give estimates of the entropy change near the transition. This estimate is done via the Clapeyron equation,

$$\Delta S = P_s^2 / 2\epsilon_0 C, \quad (21)$$

where C is the Curie constant in the Curie-Weiss expression for the relative dielectric constant

$$K' = C / (T - T_0). \quad (22)$$

If we use $C = 1.4 \times 10^3 \text{ K}$ and $P_s = 2 \times 10^{-7} \text{ C cm}^{-2}$ and a molar volume of about $40 \text{ cm}^3 \text{ mol}^{-1}$, the entropy change is only $\Delta S/R = 8 \times 10^{-4}$. Such a change would be too small for useful refrigeration, but further measurements of LTT would be useful.

There also exists means to lower the transition temperature of order-disorder materials. There are a couple of methods whereby this can be done. One method uses hydrostatic pressure to lower the transition temperature and the other uses an electric field bias on an antiferroelectric material. Samara⁹⁸ has measured the transition temperature as a function of pressure for the ferroelectric material KH_2PO_4 and the antiferroelectric material $\text{NH}_4\text{H}_2\text{PO}_4$. The transition temperatures decrease to 0 K at 17 kbar for KH_2PO_4 and 33 kbar for $\text{NH}_4\text{H}_2\text{PO}_4$. The transition temperatures in zero pressure are 122 K for KH_2PO_4 and 151 K for $\text{NH}_4\text{H}_2\text{PO}_4$. What happens then to the transition entropy, or the dipolar entropy, as the transition temperature is lowered? To answer this we use the Clapeyron equation,

$$\Delta S = \Delta v \frac{dp}{dT_c}, \quad (23)$$

where Δv is the change in molar volume at the transition from the ferroelectric to the paraelectric state and dp/dT_c is the slope of the pressure vs temperature curve separating the two phases. At $p = 0$ the entropy change is⁶⁴ $\Delta S/R = 0.37$. This number is used with Samara's⁹⁸ value for dp/dT at $p = 0$. Then if Δv is assumed independent of temperature, we get the following expression for the entropy change below 50 K by using Samara's data for T_c vs p :

$$\Delta S/R = 6.0 \times 10^{-3} T_c. \quad (24)$$

At $T_c = 5 \text{ K}$ the entropy change is then $\Delta S/R = 3 \times 10^{-2}$, which is sufficiently high for a refrigerator. For $\text{NH}_4\text{H}_2\text{PO}_4$

we expect the entropy change at 5 K to be about $\Delta S/R = 2 \times 10^{-2}$. Because $\text{NH}_4\text{H}_2\text{PO}_4$ is antiferroelectric, it would not have the problem of hysteresis as long as the applied field does not cause a change of state. However, the need for a pressure of 33 kbars probably makes such a method impractical.

In the case of an antiferroelectric, such as $\text{NH}_4\text{H}_2\text{PO}_4$, an electric field also reduces the transition temperature. For that case the Clapeyron equation is

$$\Delta S = -P_s \frac{dE}{dT_c}, \quad (25)$$

where P_s is the sublattice polarization and E is the electric field along the phase line between the antiferroelectric to the paraelectric state. No data exists for dE/dT_c , but we assume it falls off linearly with temperature below about 50 K, just as for the case of dp/dT_c . At 5 K we then expect the entropy change to be about $\Delta S/R = 2 \times 10^{-2}$. The field necessary to lower the transition to 5 K may be of the order of 100 kV cm^{-1} . The application of a field to an antiferroelectric in some cases may introduce a ferroelectric state between the antiferroelectric and paraelectric states. If the induced ferroelectric state does occur in $\text{NH}_4\text{H}_2\text{PO}_4$, the entropy change at 5 K would be reduced, but the field required to push the transition down to 5 K would also be reduced. A study of $\text{NH}_4\text{H}_2\text{PO}_4$ in an electric field would be very desirable in establishing its usefulness as a refrigerator material.

For a material to have a zero-field transition to a ferroelectric or antiferroelectric state at a very low temperature requires a small dipole moment. In fact the transition temperature will be proportional to the square of the distance between ions. At some point the zero point motion of the atoms would tend to make smaller displacements, and hence lower transition temperatures, unstable. Kurtz⁹⁹ has shown that 20 K is an approximate cut-off temperature below which a transition to a dielectrically ordered state cannot occur. Naturally a lower transition could occur in dilute materials, but the entropy per unit volume is also decreased by the dilution.

As mentioned earlier, the doped alkali halides such as $\text{KCl} : \text{OH}$ and $\text{RbCl} : \text{CN}$ have been used for cooling at temperatures below 1 K. These are order-disorder materials and the entropy change from the ordered state to the disordered (paraelectric) state is $R \ln 6$. This change, however, is on a mole basis for the OH or CN dopant. Since these materials are doped to only about $5 \times 10^{18} \text{ cm}^{-3}$, the refrigeration power per unit volume is rather small, although the material remains in the disordered state down to temperatures below 1 K. At temperatures above 1 K the lattice heat capacity of the host material is so large that the electrocaloric cooling effects become too small to be of any use for refrigeration. If the concentration for dipoles can be increased to at least 10^{20} cm^{-3} , refrigeration in the 4-15 K temperature range with these materials may be practical if high enough fields can be reached without breakdown. Some effort along this line is now in progress.¹⁰⁰ The problem to overcome in this approach is the clustering of the dopant dipoles when the

concentration becomes high. Since clustering is an ordering mechanism, the dipolar entropy is partially or entirely removed even at room temperature. It is uncertain whether a dipole concentration of 10^{20} cm^{-3} can be achieved without clustering and without significantly raising the ordering temperature, but this line of research should be pursued further.

Finally we should mention the possibility of refrigeration with materials which have a coupling between a magnetic spin system and an electric-dipole system. In such materials an electric field can change the entropy of the magnetic spin system. If the coupling is strong enough and the magnetic ordering temperature is below 4 K, then such a material could provide practical electrocaloric refrigeration at 4 K. A study of such materials would be useful.

Conclusions

This study showed that the SrTiO_3 glass-ceramics and doped ceramics have more pronounced peaks in the dielectric constant vs temperature curves than do the other nominally pure dielectric materials studied. The positive slope at temperatures below the peak cannot be used for electrocaloric refrigeration as originally believed. The fundamental thermodynamic quantity, the dc polarization, had only negative values for $\partial P/\partial T$ when the sample was cooled in the applied field. The slope was nearly zero for temperatures below about 5 K in all samples tested. It was concluded that the peaks in the dielectric constant were a result of the thermal electret behaviour of impurity-vacancy dipoles.

Electrocaloric cooling effects could be seen in many of the samples tested for the temperature range 10–30 K where $\partial P/\partial T$ is large and negative. The largest effects were seen in SrTiO_3 ceramics, rather than glass-ceramics, with similar effects seen in a KTaO_3 single crystal. The observed cooling effects were the order of 0.3 K or less for fields of 20 kV cm^{-1} . Such effects were not large enough for a practical refrigerator, although the fields were not very high.

In this study, glass-ceramics, ceramics and single crystals were investigated to better understand the general principles of dielectric behaviour and to search for possible cooling materials. All of the materials studied for possible cooling effects were of the soft optic phonon mode (displacive) type dielectrics. Theoretical calculations of the thermodynamic quantities using the phonon dispersion curves were made and showed good agreement with the experimental results. From these calculations it was concluded that the entropy in such materials is too small for practical refrigeration at 4 K even with infinitely high electric fields. However, discovery of a material with a low Debye temperature and a large TO–TA mode interaction would warrant further investigation.

Dielectric materials of the order-disorder type have orders of magnitude higher entropy ($\Delta S/R \approx 1$) in the paraelectric state than do the displacive type materials at low temperatures. Unfortunately, an order-disorder dielectric with a low enough transition temperature has not been found. It is recommended that the material lithium thallium tartrate,

which has anomalous dielectric behaviour at 11 K, be investigated further. Further low temperature studies are also needed on $\text{NH}_4\text{H}_2\text{PO}_4$, which from theoretical estimates could have enough entropy change remaining at 5 K in a high field to make a useful refrigerator. The doping of certain materials with OH or CN dipoles to levels of 10^{20} cm^{-3} may also prove fruitful.

Both mechanical and magnetothermal types of heat switches can be used successfully for a cyclic refrigerator operating between 15 and 4 K. Multiple leaf contact switches are useful for loads up to the order of 5 WK^{-1} . The magnetothermal switches, where a transverse magnetic field alters the thermal conductivity of a metal single crystal, are particularly useful because they have no moving parts. Single crystal beryllium can be used for both the upper and lower switch. It is possible to use tungsten, but for the lower switch only.

Further engineering work on an electrocaloric refrigerator is not practical at this time. Instead more basic research on the thermodynamic behaviour of dielectrics must be done to find a suitable refrigeration material or to show that such a material cannot exist for certain fundamental reasons.

The authors are grateful to Dr G.A. Samara of the Sandia Laboratories for kindly loaning the KTaO_3 and TlBr single crystals and PZT ceramics, and to Dr H. Holland and Mr J. Sage of the Corning research Laboratory for assistance with x-ray analyses and sample preparation. Thanks are also due to Mrs B. Bender of NBS–Boulder for help with the computer processing of data.

References

- 1 Strobridge, T.R. Nat Bur Stand US Tech Note 655 (1974)
- 2 Lawless, W.N. Proc Cryo Cooler Conf Tech Report AFFDL-TR-73-149 1 (1973) 417
- 3 Lawless, W.N. *Rev Sci Instrum* **42** (1971) 561
- 4 Rubin, L.G., Lawless, W.N. *Rev Sci Instrum* **42** (1971) 571
- 5 Lawless, W.N., Radebaugh, R., Soulen, R.J. *Rev Sci Instrum* **42** (1971) 567
- 6 Lawless, W.N. *J Opt Soc Am* **62** (1972) 1449; *J Opt Soc Am* **64** (1974) 820
- 7 Lawless, W.N. US Patent No 3 638 440 (1972)
- 8 Garrett, C.G.B. *Magnetic Cooling* (John Wiley and Sons, Inc, New York, 1954)
- 9 Kobeko, P., Kurtschatov, J. *Zeit fur Physik* **66** (1930) 192
- 10 van Geuns, J.R. *Philips Res Rept Suppl* No 6 (1966); US Patent 3 413 814 (1968)
- 11 Steigmeier, E.F. *Phys Rev* **168** (1968) 523
- 12 See, for example, Colwell, J.H. *Rev Sci Instrum* **40** (1969) 1182, and references cited therein
- 13 Berman, R. *J Appl Phys* **27** (1956) 318
- 14 Berman, R., Mate, C.F. *Nature* **182** (1958) 1661
- 15 Siegwarth, J.D. *Cryogenics* **16** (1976) 73
- 16 Engels, L.M.L., Gorter, F.W., Miedema, A.R. *Cryogenics* **12** (1972) 141
- 17 DeHaas, W.J., DeNobel, J. *Physica* **5** (1938) 449; DeNobel, J. *Physica* **23** (1957) 261
- 18 Long, J.R. *Phys Rev* **B3** (1971) 1197
- 19 Radebaugh, R. *J Low Temp Physics* **27** (1977) 91
- 20 Gruneisen, E., Adenstedt, H. *Ann Physik* **5** 31 (1938) 714
- 21 Lawless, W.N. *J Phys Chem Solids* **30** (1969) 1161
- 22 Weiss, P., Forrer, R. *Ann Phys* (Paris) **5** (1926) 153
- 23 Thacher, P.D. *J Appl Phys* **39** (1968) 1996, and references cited therein
- 24 Granicher, H. *Helv Phys Acta* **29** (1956) 210

- 25 Franzel, C., Gladun, A., Gladun, C., Hegenbarth, E., Knorn, M. *Phys Stat Sol (a)* 15 K61 (1973)
- 26 Barrett, J.H. *Phys Rev* 86 (1952) 118
- 27 Hegenbarth, E. *Cryogenics* 1 (1961) 242
- 28 Kikuchi, A., Sawaguchi, E. *J Phys Soc Japan* 19 (1964) 1497
- 29 Hegenbarth, E. *Phys Stat Sol* 8 (1965) 59
- 30 Sawaguchi, E., Kikuchi, A., Kodera, Y. *J Phys Soc Japan* 17 (1962) 1666
- 31 Kanzig, W., Hart, H.R., Jr., Roberts, S. *Phys Rev Letters* 13 (1964) 543
- 32 Kuhn, U., Luty, F. *Solid State Commun* 4 (1965) 31
- 33 Shepherd, L., Feher, G. *Phys Rev Letters* 15 (1965) 194; Shepherd, I.W. *J Phys Chem Solids* 28 (1967) 2027
- 34 Lawless, W.N. *J Appl Phys* 40 (1969) 4448
- 35 Lombardo, G., Pohl, R.O. *Phys Rev Letters* 15 (1965) 291
- 36 Pohl, R.O., Taylor, V.L., Gouban, W.M. *Phys Rev* 178 (1969) 1431
- 37 Korrovits, V.Kh., Luud'ya, G.G., Mikhkel'soo, V.T. *Cryogenics* 14 (1974) 44
- 38 Lawless, W.N. US Patent 3 436 924 (1969)
- 39 Robinson, M.C., Wertheimer, M.R. US Patent 3 650 117 (1972)
- 40 Lang, S.B. *Ferroelectrics* 11 (1976) 519
- 41 Lang, S.B. *Phys Rev B* 4 (1971) 3603
- 42 Radebaugh, R. *Phys Rev Letters* 40 (1978) 572
- 43 Herczog, A. *J Amer Ceram Soc* 47 (1964) 107; Layton, M.M., Herczog, A. *ibid* 50 (1967) 369
- 44 Radebaugh, R., Siegwarth, J.D., Lawless, W.N., Morrow, A.J. Electrocaloric Refrigeration for Superconductors, Nat Bur Std Tech Report NBSIR 76-847 (1977)
- 45 Lawless, W.N., Morrow, A.J. *Ferroelectrics* 15 (1977) 167
- 46 Samara, G.A., Morosin, B. *Phys Rev B* 8 (1973) 1256
- 47 Siegwarth, J.D., Morrow, A.J. *J Appl Phys* 47 (1976) 4784
- 48 Gesi, K. *J Phys Soc Japan* 33 (1972) 108
- 49 Lawless, W.N. *Phys Rev B* 14 (1976) 134
- 50 Colwell, J.H. private communication, 1975
- 51 Siegwarth, J.D. *J Appl Phys* 48 (1977) 1
- 52 Neville, R.C., Hoeniesen, B., Mead, C.A. *J Appl Phys* 43 (1972) 2124
- 53 Lawless, W.N., Morrow, A.J. *Ferroelectrics* 15 (1977) 159
- 54 Siegwarth, J.D., Holste, J.C., Morrow, A.J. *J Appl Phys* 47 (1976) 4791
- 55 Lawless, W.N. *Phys Rev* 16 (1977) 433
- 56 Hulm, J.K. *Phys Rev* 92 (1953) 504
- 57 Siegwarth, J.D., Lawless, W.N., Morrow, A.J. *J Appl Phys* 47 (1976) 3789
- 58 Sawaguchi, E. *J Phys Soc Japan* 8 (1953) 615
- 59 Samara, G.A. *Phys Rev* 165 (1968) 959
- 60 Holste, J.C., Lawless, W.N., Samara, G.A. *Ferroelectrics* 11 (1976) 337
- 61 Weaver, H.E., *J Phys Chem Solids* 11 (1959) 274
- 62 Burke, W.J., Pressley, R.J. *Solid State Commun* 9 (1971) 191
- 63 Saifi, M.A., Cross, L.E. *Phys Rev* 82 (1970) 677
- 64 Jona, F., Shirane, G. *Ferroelectric Crystals* Macmillan, New York, (1962) 251
- 65 Hulm, J.K., Matthias, B.T., Long, E.A. *Phys Rev* 79 (1950) 885
- 66 Demurov, D.G., Venevtsev, Yu.N. *Sov Phys Solid State* 13 (1971) 553 [*Fiz Tverd Tela* 13 (1971) 669]
- 67 Bucci, C., Fieschi, R., Guidi, G. *Phys Rev* 148 (1966) 816
- 68 Cook, J.S., Dryden, J.S. *Proc Phys Soc (London)* 80 (1962) 479
- 69 Crawford, J.H., Jr. *J Phys Chem Solids* 31 (1970) 399
- 70 Stoebe, T.G., Watanabe, S. *Phys Stat Sol (a)* 29 (1975) 11
- 71 Fiory, A.T. *Phys Rev B* 4 (1971) 614; Lawless, W.N. *Phys Kondens Materie* 5 (1966) 100
- 72 Radebaugh, R. Proc Conf on Application of Closed-Cycle Cryocoolers to Small Superconducting Devices, Boulder, Nat Bur Std, Special Publication 508, 7
- 73 Blinc, R., Zeks, B. Soft modes in ferroelectrics and antiferroelectrics, selected topics in solid state physics, Vol 13 North-Holland, New York (1974)
- 74 Cochran, W. *Adv Phys* 9 (1960) 387; *Adv Phys* 10 (1961) 401
- 75 Anderson, P.W. Proceedings of the Conference on the Physics of Dielectrics (Academy of Science, USSR, Moscow, 1958) 290
- 76 Burns, G., Scott, B.A. *Phys Rev B* 7 (1973) 3088
- 77 Ziman, J.M. Principles of the Theory of Solids, 2nd Ed (Cambridge University Press, 1972)
- 78 Donnelly, R.J., Roberts, P.H. *J Low Temp Physics* 27 (1977) 687
- 79 Yamada, Y., Shirane, G. *J Phys Soc Japan* 26 (1969) 396
- 80 Bell, R.O., Rupprecht, G. *Phys Rev* 129 (1963) 90
- 81 Worlock, J.M., Fleury, P.A. *Phys Rev Letters* 19 (1967) 1176; Fleury, P.A., Worlock, J.M. *Phys Rev* 174 (1968) 613
- 82 Shirane, G., Yamada, Y. *Phys Rev* 177 (1969) 858
- 83 Cowley, R.A. *Phys Rev A* 134 (1964) 981
- 84 Hegenbarth, E. *Phys Stat Sol* 2 (1962) 1544
- 85 Todd, S.S., Lorenson, R.E. *J Amer Chem Soc* 74 (1952) 2043
- 86 Peressini, P.P., Harrison, J.P., Pohl, R.O. *Phys Rev* 182 (1969) 939
- 87 Shirane, G., Nathans, R., Minkiewicz, V.J. *Phys Rev* 157 (1967) 396
- 88 Axe, J.D., Harada, J., Shirane, G. *Phys Rev B* 1 (1970) 1227
- 89 Barrett, H.H. *Phys Letters* 26A (1968) 217
- 90 Cowley, E.R., Okazaki, A. *Proc Roy Soc (London)* A300 (1967) 45
- 91 Morse, G.E., Lawson, A.W. *J Phys Chem Solids* 28 (1967) 939
- 92 Khmel'nitskii, D.E., Sheneerson, V.L. *Sov Phys-JETP* 37 (1973) 164
- 93 Devonshire, A.F. *Adv Phys* 3 (1954) 85
- 94 Matthias, B.T., Hulm, J.K. *Phys Rev* 82 (1951) 108
- 95 Sawaguchi, E., Cross, L.E. *Appl Phys Letters* 18 (1971) 1; *Ferroelectrics* 3 (1972) 327
- 96 Sawaguchi, E., Cross, L.W. *Ferroelectrics* 2 (1971) 37
- 97 Abe, R., Kamiya, N., Matsuda, M. *Ferroelectrics* 8 (1974) 557
- 98 Samara, G.A. *Phys Rev Letters* 27 (1971) 103
- 99 Kurtz, S.K. Electro-optic Materials, Trans Amer Crystallographic Assoc, Vol II on Appl Crystal Chem (1975)
- 100 von Molnar, S. private communication (1977)